

8-31-1991

## Measurement of the electrical and optical properties of Thermid polyimide

Zhixiong Zhu  
*New Jersey Institute of Technology*

Follow this and additional works at: <https://digitalcommons.njit.edu/theses>



Part of the [Electrical and Electronics Commons](#)

---

### Recommended Citation

Zhu, Zhixiong, "Measurement of the electrical and optical properties of Thermid polyimide" (1991).  
*Theses*. 2694.  
<https://digitalcommons.njit.edu/theses/2694>

This Thesis is brought to you for free and open access by the Electronic Theses and Dissertations at Digital Commons @ NJIT. It has been accepted for inclusion in Theses by an authorized administrator of Digital Commons @ NJIT. For more information, please contact [digitalcommons@njit.edu](mailto:digitalcommons@njit.edu).

## **Copyright Warning & Restrictions**

The copyright law of the United States (Title 17, United States Code) governs the making of photocopies or other reproductions of copyrighted material.

Under certain conditions specified in the law, libraries and archives are authorized to furnish a photocopy or other reproduction. One of these specified conditions is that the photocopy or reproduction is not to be “used for any purpose other than private study, scholarship, or research.” If a user makes a request for, or later uses, a photocopy or reproduction for purposes in excess of “fair use” that user may be liable for copyright infringement,

This institution reserves the right to refuse to accept a copying order if, in its judgment, fulfillment of the order would involve violation of copyright law.

**Please Note: The author retains the copyright while the New Jersey Institute of Technology reserves the right to distribute this thesis or dissertation**

Printing note: If you do not wish to print this page, then select “Pages from: first page # to: last page #” on the print dialog screen

The Van Houten library has removed some of the personal information and all signatures from the approval page and biographical sketches of theses and dissertations in order to protect the identity of NJIT graduates and faculty.

# ABSTRACT

Title of Thesis: Measurement of the Electrical and Optical Properties of THERMID Polyimide

Zhixiong Zhu, Master of Science, Electrical Engineering Dept., 1991

Thesis directed by: Dr. K. Ken. Chin, Associate Professor, Physics Dept.

Electrical and optical properties of spin-coated THERMID polyimide EL-5010 have been studied and evaluated in this thesis. The D.C. bulk resistivities of 0.96-2.56  $\mu\text{m}$  thick samples were measured to be  $10^{16} \Omega\text{-cm}$  over the 27-160°C range using a test system consisting of Keithley 236 Source-Measure Unit. The bulk resistivity decreased to  $2 \times 10^{14} \Omega\text{-cm}$  at 200°C. The surface resistivity,  $10^{15} \Omega/\square$ , and breakdown voltage, 350 V/ $\mu\text{m}$ , were also measured. The fixed charge concentration and mobile ion concentration in the THERMID polyimide EL-5010 insulator of a MIS capacitor structure were measured using a high frequency C-V measurement technique. The measured value of the positive mobile ion concentration was  $1.12 \times 10^{11} \text{cm}^{-2}$  and of the fixed charge was found to be negative with a value of  $10^{11} \text{cm}^{-2}$ . The transmission spectrum over the wave number range of 1-10  $\text{cm}^{-1}$  was obtained using

a test system consisting of a mercury lamp, a lamellar grating, and a dip-stick helium-cooled bolometer. The transmission spectrum for the wave number range of 10-60  $\text{cm}^{-1}$  was obtained using a test system consisting of a Synchrotron far infrared light source, a Nicolet Michelson scanning spectrometer, and a pumped helium-cooled detector. In the wave number range of 1-25  $\text{cm}^{-1}$ , the far infrared absorption of the THERMID polyimide EL-5010 increased with the increasing of wave number and reached the maximum at wave number 25 $\text{cm}^{-1}$ . In the wave number range of 25-60  $\text{cm}^{-1}$ , almost no transmission occurred. Mechanisms responsible for these electrical and optical properties are discussed.

2/ **MEASUREMENT OF THE  
ELECTRICAL AND OPTICAL PROPERTIES  
OF THERMID POLYIMIDE**

1/ by  
Zhixiong Zhu

Thesis submitted to the Faculty of the Graduate School of  
the New Jersey Institute of Technology  
in partial fulfilment of the requirements for the degree of  
Master of Science in Electrical Engineering

1991



# VITA

Name: Zhixiong Zhu

Permanent Address:

Degree and date to be conferred: MSEE, 1991

Date of birth:

Place of birth:

Secondary education: High School, Shanghai, P.R.China

Collegiate institutions attended	Dates	Degree	Date of Degree
Shanghai Jiao Tong University	1978-1982	BSEE	1982
NJIT	1989-1991	MSEE	1991

Major: Electrical Engineering

## ACKNOWLEDGMENTS

I wish to express my sincere gratitude to Dr. K. Ken Chin for his valuable guidance, inspiration, and financial support during the entire course of this thesis. I would also like to express my sincere gratitude to Professor S. N. Zhao and Dr. K. D. Moller for giving their instructions and suggestions\* during the course. Without their valuable help this thesis would not have seen the light of today. Furthermore, I would like to express my sincere thanks to Dr. P.G. Jobe and C. Puglisi of National Starch & Chemical Co. for providing their precious supports and all the conveniences for our research. I am indebted to Professor G. H. Feng for his instructions and willful help in my work. I would also like to express my sincere thanks to Dr. R. Cornely, Dr. M. Sosnowski and Dr. A. Jermakian for giving their valuable time, very good suggestions and constructive criticisms. Last, but certainly not the least, I would like to acknowledge Dr. N. M. Ravindra and Mr. Nelay for providing C-V Plotter and help in C-V measurements.

# Contents

- 1. Introduction 1
  
- 2. D.C. Electrical Properties of THERMID 5
  - 2.1 Bulk Resistivity ..... 5
  - 2.2 Breakdown Voltage ..... 9
  - 2.3 Surface Resistivity ..... 14
  - 2.4 Discussion ..... 16
  
- 3. Fixed Charge and Mobile-ion in THERMID Layer 19
  - 3.1 Test Principle ..... 19
  - 3.2 Measurement Method ..... 26
  - 3.3 Sample Preparation ..... 29
  - 3.4 Test Results ..... 32
  - 3.5 Discussion ..... 36
  
- 4. Far-Infrared Absorption Properties of THERMID 37
  - 4.1 Test Principle ..... 37
  - 4.2 Test System ..... 43
  - 4.3 Measurement Method ..... 45
  - 4.4 Test Results ..... 47

4.5 Discussion .....	55
5. Summary	57
Reference	61
Appendix	63
Appendix A: Program for THERMID Resistivity Measurement .....	63
Appendix B: Program for THERMID Far-Infrared Absorption Properties Measurement .....	68

## List of Figures

1.1 Data of Controlled Film Deposition .....	4
2.1 THERMID D.C. Measurement System Schematic Diagram .....	6
2.2 Sample Schematic of THERMID D.C. Measurement .....	8
2.3 Capacitor Leakage Current Test Schematic .....	8
2.4 Applied Voltage versus Time during a d.c. Experiment.....	10
2.5 Current Response versus Time for the Applied Voltage in Fig. 2.4 .....	10
2.6 THERMID Breakdown Voltage & Surface Resistivity Measurement System Schematic Diagram .....	11
2.7-2.8 The Temperature Dependence of THERMID Bulk Resistivity .....	12
2.9-2.10 Voltage Breakdown Tests .....	13
2.11 Sample Schematic of Surface Resistivity Measurement.....	15
2.12 Surface Resistivity of THERMID at Room Temperature.....	15
2.13 Structure of THERMID EL-5010 .....	16
3.1 MIS Structure Used in the Experiment where THERMID Served as Insulator ..	19
3.2 Equivalent Circuit of the MIS Structure of Fig. 3.1 .....	20
3.3 Frequency-Dependent Equivalent Circuit of Fig. 3.2 .....	21
3.4 Equivalent Circuit of MIS under High Frequency.....	22
3.5 Principle Block Diagram of High frequency C-V Measurement .....	23

3.6 Sample Schematic for C-V Measurement of MIS with THERMID as Insulator Dielectric .....	33
3.7 C-V Curve of the MIS Before Positive Temperature-bias stress. THERMID was Used as Insulator Dielectric .....	34
3.8 C-V Curve of the MIS After Positive Temperature-bias stress. THERMID was Used as Insulator Dielectric .....	35
4.1 $S(Y) = J(Y) - \frac{1}{2} J(0)$ .....	39
4.2 Test System Schematic Diagram of Using Lamellar Grating Spectrometer to Measure Far-infrared properties of THERMID .....	44
4.3 Optical Path Difference in Experiment .....	45
4.4 Interferogram in Experiment .....	46
4.5 The Interferogram of Background (Without THERMID in Optical Path) .....	49
4.6 The Sample Interferogram (With THERMID in Optical Path) .....	50
4.7 Spectrum Obtained in Experiment .....	51
4.8 THERMID Transmission Spectrum I .....	52
4.9 THERMID Transmission Spectrum II .....	53

## List of Tables

1.1 THERMID EL (Electronic Grade) Basic Properties .....	3
2.1 Data of Bulk Resistivity Measurement at Room Temperature .....	11
3.1 Temperature-bias Procedures if Mobile ion existing in the THERMID at Room Temperature <sup>a</sup> .....	28
3.2 Ratio of $C_{min}/C_{max}$ estimated by eq.(3-20) .....	31
3.3 Constants needed by "C-V Measurement <sup>†</sup> Analysis Programs" for the C-V Measurement of the MIS Where THERMID was used as Insulator Dielectric ...	33
3.4 Data of C-V Measurement Before Positive Temperature-bias stress .....	34
3.5 Data of C-V Measurement After Positive Temperature-bias stress .....	35
4.1 Data of Fig.4-7 and Fig.4-8, Transmission Versus Wavenumber .....	54
4.2 Data of Fig.4-9, Transmission Versus Wavenumber .....	54

# Chapter 1 Introduction

High speed , high density integrated circuits are revolutionizing the microelectronics industry. Today to place as many as 300,000 transistors and 400 I/O's, equivalent of an entire minicomputer, on a single monolithic silicon chip is possible.<sup>[1]</sup>

Mainly because of these ULSI devices, ultra-fast computers and telecommunication systems have become available. However such IC circuits have created many problems for present packing technology. In fact, many of the on-chip benefits gained by VLSI are now lost during packaging which uses the technology of multilayer and hybrid circuits.<sup>[2]</sup> A technology that can accommodate greater package density and higher signal speeds is required . Recent literature shows that one of the most successful packaging technologies designed to match the requirements of today's modern IC's is applying thin film IC fabrication techniques to manufacture high-density interconnects(HDI) and multichip modules (MCM's).<sup>[3]</sup> A key to the success of this new packaging technology is the use of an organic dielectric as the interlayer.<sup>[4]</sup>

Polyimides, as organic dielectrics, are receiving more and more attention from the microelectronics industry because of their high thermal and chemical stability, good mechanical properties and excellent dielectric behavior.<sup>[5]</sup> However,

conventional high molecular weight polyimides, derived from their corresponding polyamic acids, have certain inherent weaknesses that have limited their utility.<sup>[6]</sup>

Now acetylene-terminated polyimide oligomers, developed by the National Starch & Chemical Corp. and commercialized under the trade name "THERMID", offer an alternative. They maintain all the superior final properties of polyimides while dramatically improving their overall processability as a coating material. For the HDI process engineer, THERMID has shown a high degree of planarization, excellent adhesion, and very good ability to attain and maintain a low dielectric constant in service.<sup>[6]</sup>

Actual HDI devices which use THERMID as the interlevel dielectric, for example an HDI module which interconnects eight S-RAM chips<sup>[6]</sup>, have been reported to be very successful. The electrical and optical properties of THERMID, however, have not been completely measured and studied. Under a project sponsored by National Starch & Chemical Co., a series of experiments and evaluations of THERMID electrical and optical characteristics have been done.

This thesis reports part of the results of our recent electrical and optical studies and evaluations of THERMID EL(electronic grade)-5010 as well as the experiments, processes, and computer programs. Some of these studies have never been done before. In these investigations, we experimentally determined the D.C. properties ( bulk resistivity, surface resistivity and breakdown voltage ) of THERMID. We also studied the surface electrical properties of THERMID thin films when they are used as insulator layers in metal-insulator-semiconductor(MIS) structures. This was done by capacitance-voltage(C-V) measurements and

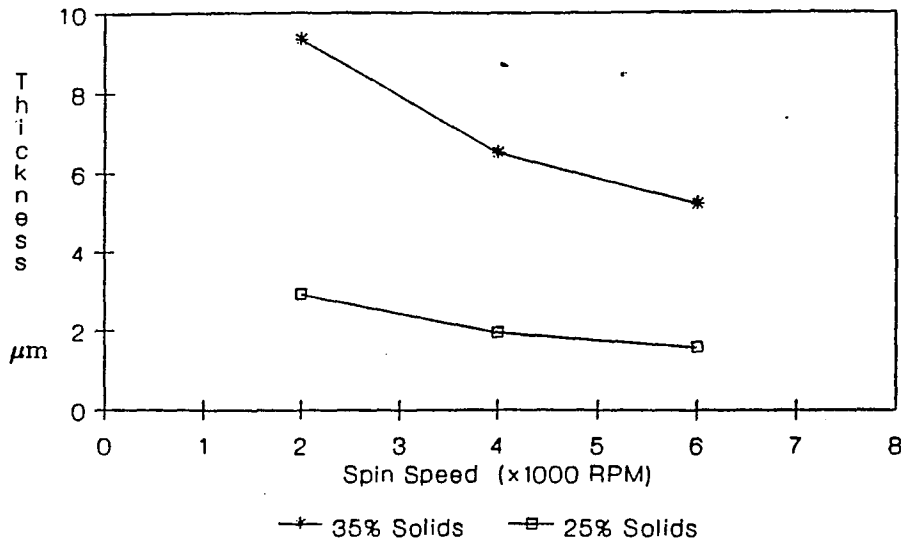
calculations of the fixed charge and mobile-ion concentration. The far infrared optical properties of THERMID were also studied by far infrared absorption measurements. These data gave a satisfactory explanation of the success of THERMID when used as a dielectric interlayer in HDI technology. They can also lead to possible future applications, such as using THERMID in optical devices for the far-infrared region.

As an end of this introduction, some basic physical properties of THERMID films, parameters for THERMID film deposition, and typical etch conditions and etch rates are shown in table 1-1, fig.1-1, and table 1-2 respectively. These results were determined previously by the National Starch & Chemical Co..

	<u>EL-5010</u>	<u>EL-5512</u>
Viscosity (25°C, cps)	1500	1100
Solids (%)	35	47
Glass Transition Temp. (T <sub>g</sub> , DSC, °C)	214	225-230
Refractive Index	1.78	1.82
Thermal Coef. of Expansion (TCE, TMA, ppm/°C)	38	38
Tensile Strength (Kpsi)	22	21
Elastic Modulus (Kpsi)	430	420
Elongation (%)	>7	6
Yield Strength (Kpsi)	22	--

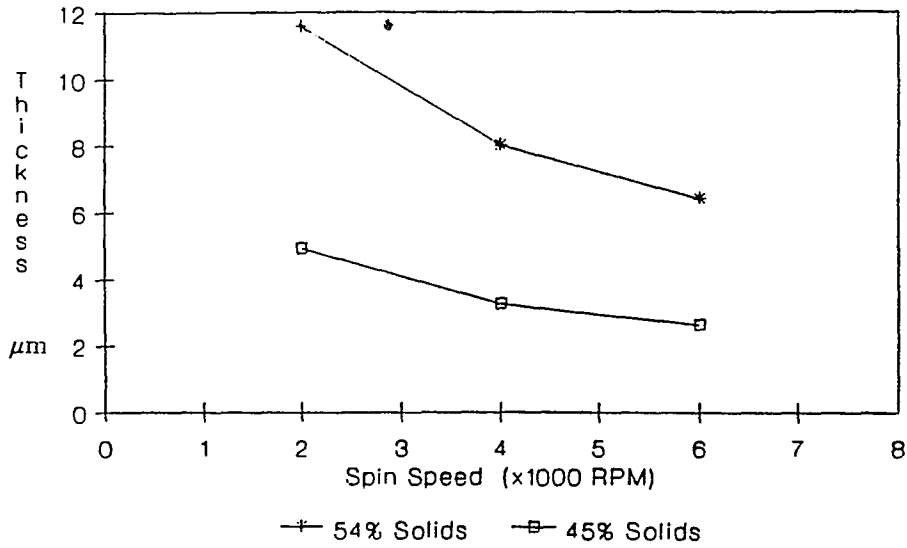
Table 1-1\* THERMID EL(electronic grade) Basic Properties

**Thickness vs. Spin Speed  
Therimid EL-5010**



On 3" Silicon Wafer  
Cured 180 C/30'; 300 C/60'; 400 C/15'

**Thickness vs. Spin Speed  
Therimid EL-5501**



On 3" Silicon Wafer  
Cured 180 C/30'; 300 C/60'; 400 C/15'

**Fig. 1-1\* Data of Controlled Film Deposition**

## Chapter 2 D.C. Electrical Properties of THERMID

### 2.1 Bulk Resistivity

#### 2.1.1 Test System

In order to measure the very high bulk resistivity and surface resistivity of THERMID, a special test system was designed. A Keithley 236 Source-Measure Unit, which can measure current as small as 10 fA ( $10^{-14}$ A) DC was used as the voltage source and current measurement equipment during testing. Special test fixture which can effectively decrease the noise level<sup>\*</sup> was designed to hold the sample being measured. The temperature of this test fixture can be controlled and monitored by using a D.C. heating coil and a type E thermocouple. The connections between the Keithley 236 and the test fixture were via triax connectors and triax cables which provided double shielding for the test signals.

The measurement was under the control of an IBM 386 AT personal computer via an IEEE 488 communication port. Data obtained by the Keithley 236 were sent to the PC, and then processed, plotted and printed. The system control and data processing program were written in Quick Basic Language. (See Appendix A.)

The system schematic is shown in Fig.2-1.

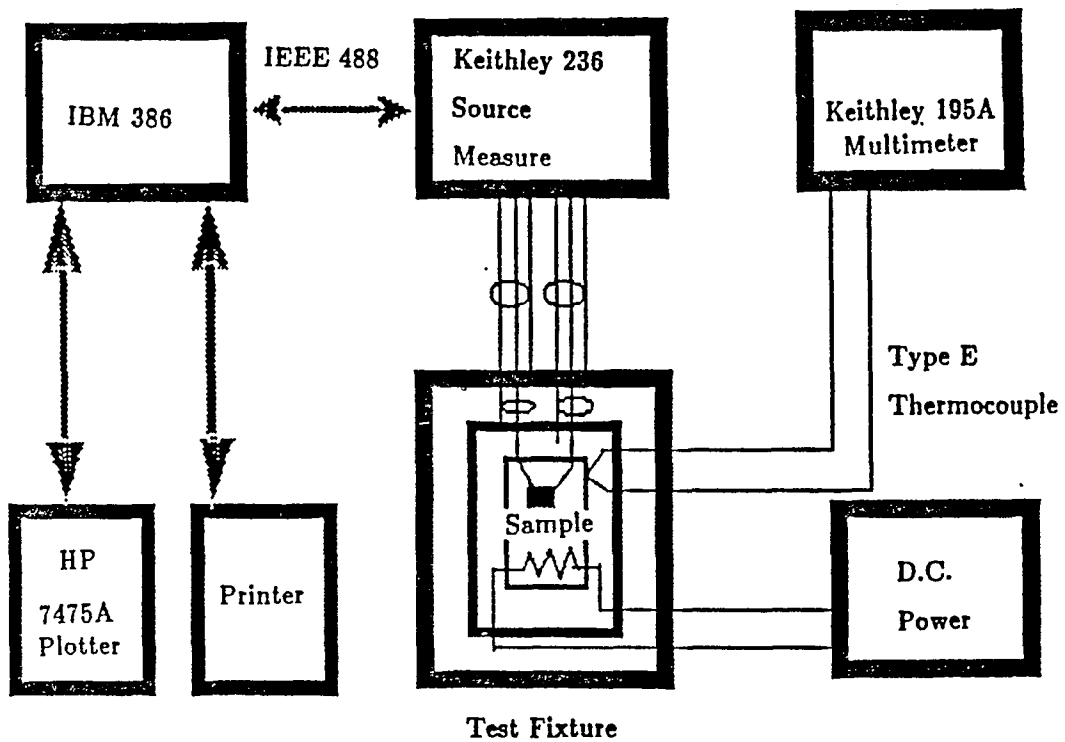


Fig. 2-1 THERMID D.C. Measurement System Schematic Diagram

### 2.1.2 Sample Preparation

For testing the D.C. properties, p-type Si wafers with resistivities of about 10-12 ohm-cm were used. All wafers were cleaned by using RCA technique<sup>[8]</sup> followed by a HF dip and thorough rinsing with deionized water. All microelectronic processing operations were performed in a class 100 clean room facility. The THERMID EL-5010 formulation was provided by National Starch & Chemical Co.. In the clean room of the company, each Si wafer was coated with the THERMID thin film strictly following the technology given by the company. The curing temperature and time were 180°C (30 minutes), 300°C (60 minutes), and 400°C (15 minutes).<sup>[7]</sup> The back of the wafer was then sanded to get off the SiO<sub>2</sub> and deposited with a layer of aluminum thin film so that a good ohmic contact with a copper plate was made. This copper plate served as negative electrode in the test. On the top of the THERMID film, aluminium and indium spots were deposited and their dimensions were measured. These spots served as positive electrodes in the test as shown in Fig 2-2. The sample was then put in the test fixture and double shielded from the outside world

### 2.1.3 Measurement method

The sample as shown in Fig 2-2 can be treated as a capacitor with the THERMID as its dielectric. The bulk resistivity of the THERMID can then be obtained by measuring the leakage current of the capacitor.<sup>[9]</sup> Fig. 2-3 shows the test configuration for the capacitor leakage current test. Once the leakage current  $I$  is known, the bulk resistivity  $\rho$  can easily be calculated from the applied voltage  $V$  and other related test parameters using the equation:

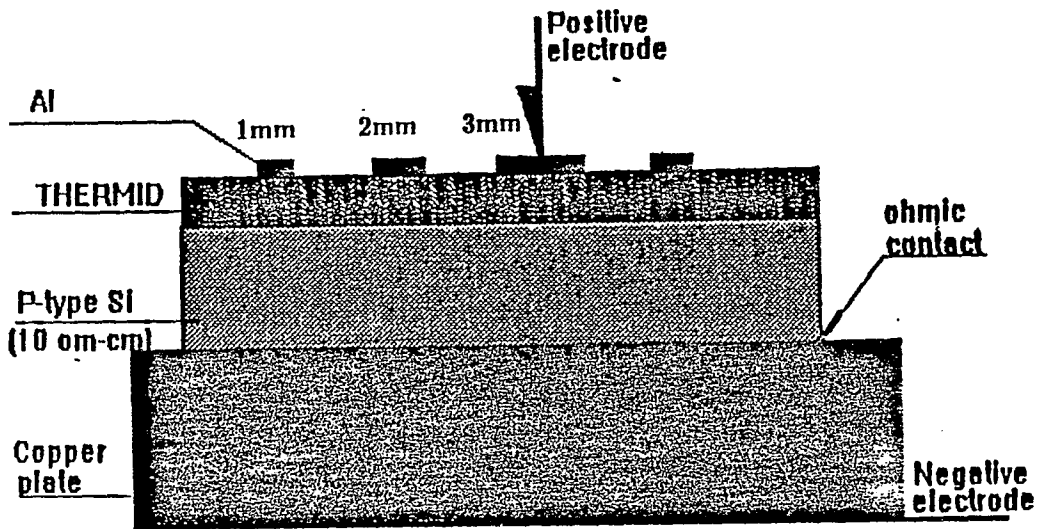


Fig. 2-2 Sample Schematic of THERMID D.C. Measurement

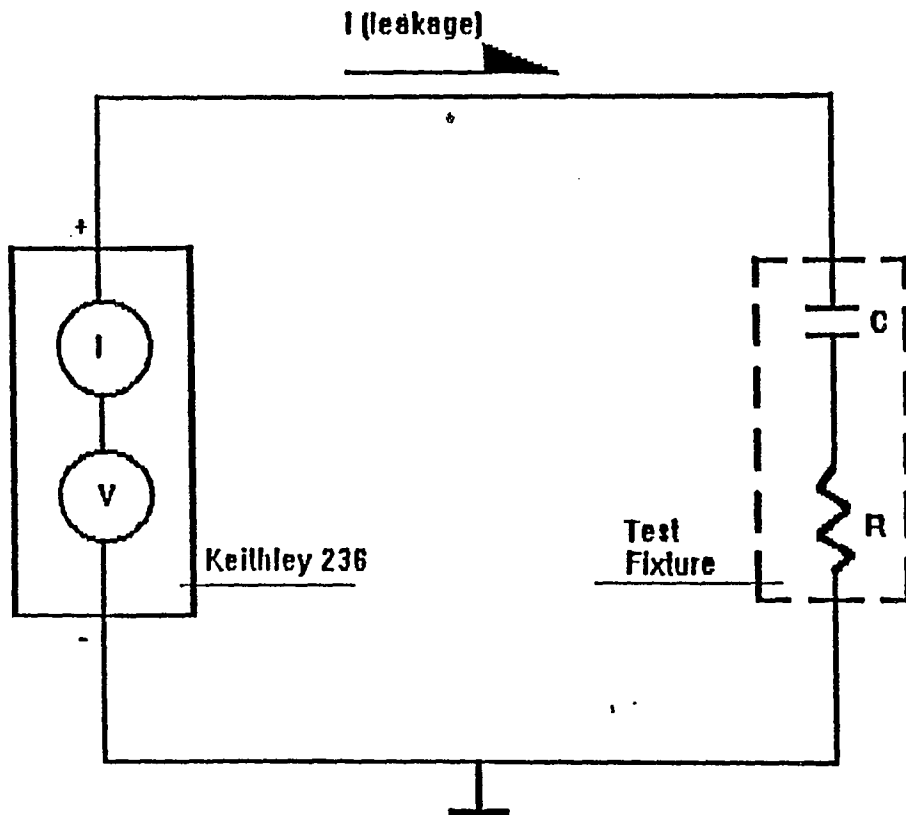


Fig. 2-3 Capacitor Leakage Current Test Schematic

$$\rho = \frac{VA}{ID} \quad (2-1)$$

where  $A$  = the area of the contact

$D$  = the thickness of the THERMID film.

Since the resistivity of the THERMID film is very high, the resistance of the Si can be neglected. An important consideration that ensure accurate results was that after the voltage was applied to the capacitor, the capacitor must be allowed to be fully charged (this will be discussed further in section 2.4) before the leakage current measurement is made. Attached T-V and T-I curves (Fig 2-4 and Fig 2-5) clearly reflected this fact. Only the last current measurement point of each corresponding step voltage in T-I curve was used to calculate bulk resistivity.

#### 2.1.4 Test results

The measurements revealed that the room temperature bulk resistivity of THERMID EL-5010 films of thicknesses of 0.96 - 2.56  $\mu\text{m}$  is no less than  $1 \times 10^{16} \Omega\text{-CM}$  as shown in table 2-1. Temperature dependence of THERMID EL-5010 bulk resistivity was also measured and the results are shown in Fig. 2-7 and Fig. 2-8.

## 2.2 Breakdown Voltage

### 2.2.1 Test System and Sample Preparation

The system schematic diagram for measuring breakdown voltage is shown in Fig. 2-6. The sample preparation procedures were similar to that described in section 2.1.2. The sample schematic is same as fig.2-2 except that the diameter of the aluminum spot was 1cm.

### 2.2.2 Measurement Method

The breakdown voltage of the THERMID thin film can be obtained by d.c.

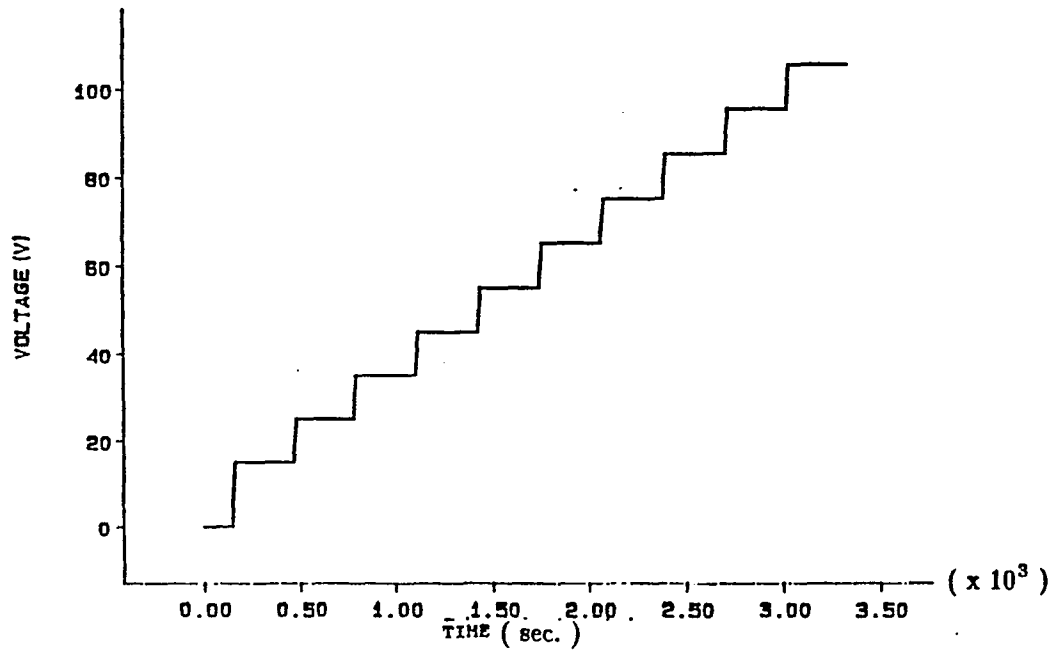


Fig. 2-4 Applied Voltage Versus Time during a d.c. Experiment

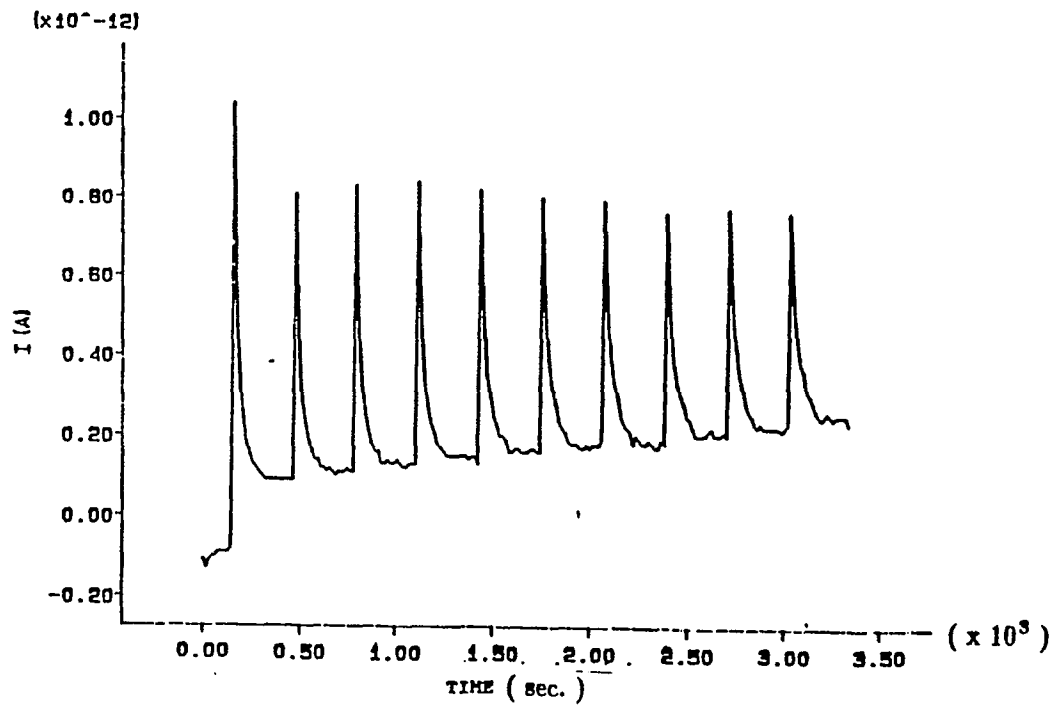


Fig. 2-5 Current Response Versus Time for the Applied Voltage in Fig. 2-4

Sample Number	Film Thickness ( $\mu\text{m}$ )	Diam. of Spot (cm)	Resistivity ( $\Omega\text{-cm}$ )
1	0.96	0.102	$5.69 \times 10^{16}$
2	0.96	0.201	$6.12 \times 10^{16}$
3	0.96	0.304	$6.01 \times 10^{16}$
4	2.56	0.201	$6.10 \times 10^{16}$
5	1.08	0.251	$5.94 \times 10^{16}$

Table 2-1 Data of Bulk Resistivity Measurement at Room Temperature

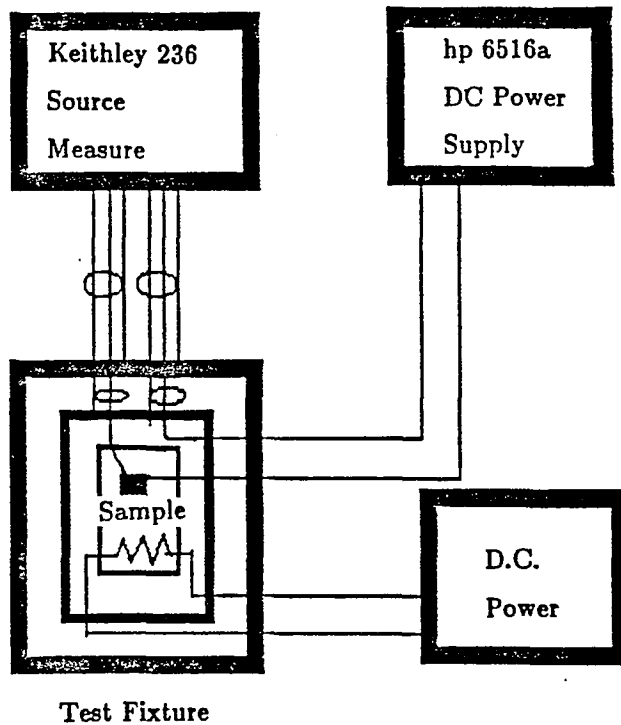


Fig. 2-6 THERMID Breakdown Voltage & Surface Resistivity Measurement System Schematic Diagram

current versus d.c. voltage measurement. The method of measuring the current was similar to that described in section 2.1.3. When the step voltage was increased to such a point that the corresponding current suddenly increased much faster than before, the breakdown occurred. After that point, decreasing step voltage could not make the current decreasing along the same path it increased before any more. That was because the breakdown of the THERMID thin film.

### 2.2.3 Test Results

The breakdown voltage of the 1  $\mu\text{m}$  THERMID EL-5010 thin film was measured to be between 180 volts to 350 volts. ( See Fig. 2-9 , Fig 2-10 , and table 2-1.)

Sample Number	Breakdown Voltage	Sample Number	Breakdown Voltage
1	348 V	4	350 V
2	200 V	5	180 V
3	350 V	6	349 V

Table 2-1 Data of Breakdown Test

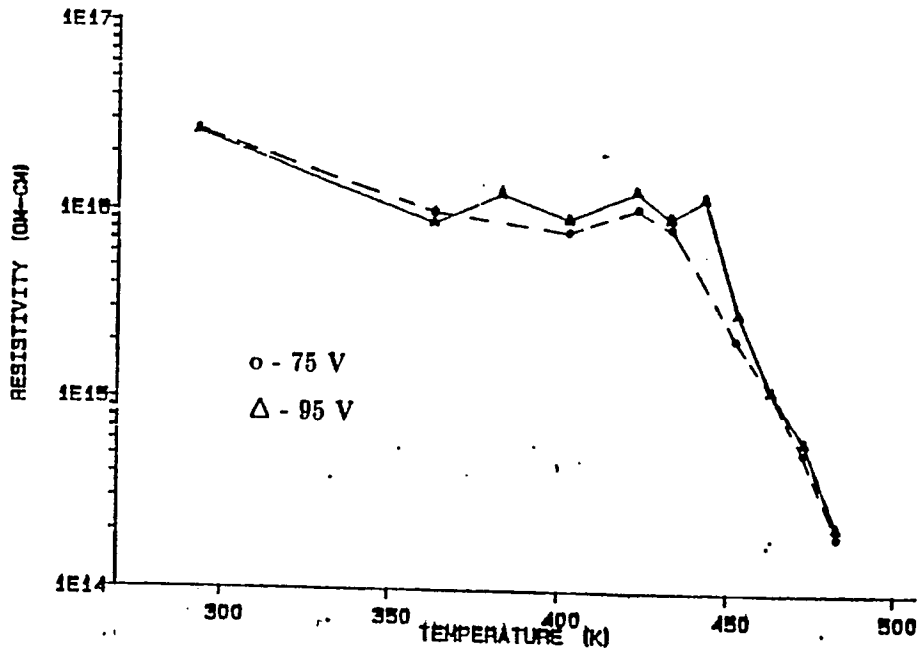


Fig. 2-7 The Temperature Dependence of Polyimide Bulk Resistivity

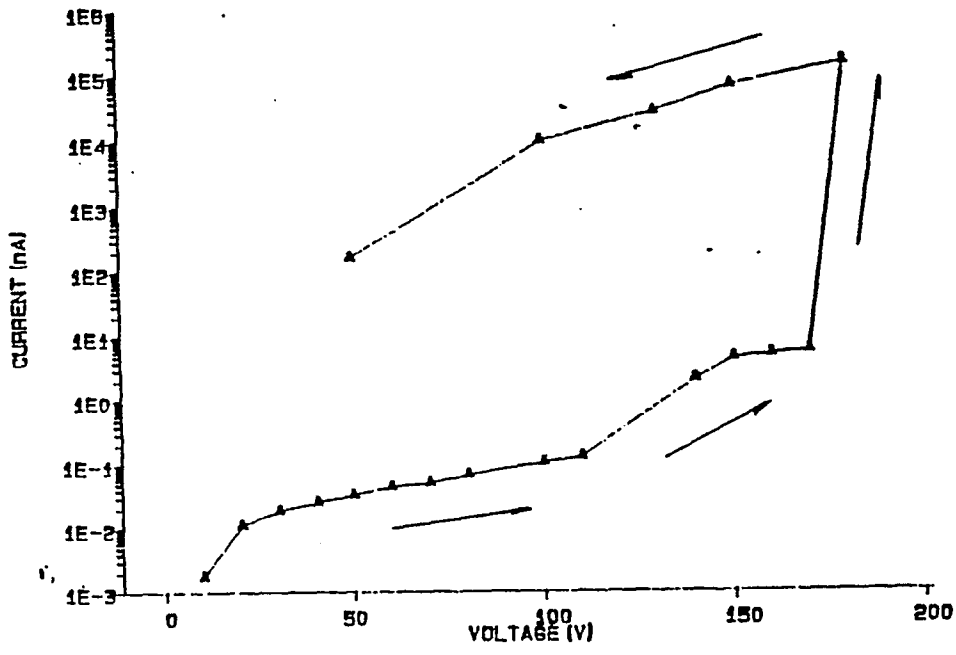


Fig. 2-9 Voltage Breakdown Tests

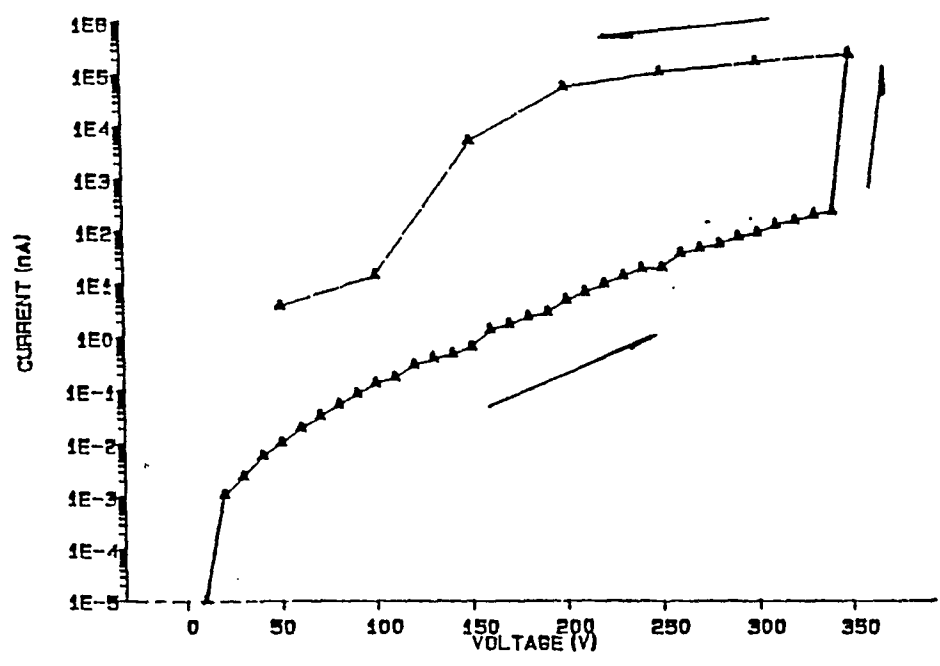


Fig. 2-10 Voltage Breakdown Tests

## 2.3 Surface resistivity

The system schematic diagram for measuring surface resistivity is shown in Fig. 2-6.

### 2.3.1 Sample preparation

For surface resistivity tests, a plate of teflon was used as a base on which about 2 mm thick layer of THERMID was coated. Before coating, the plate of teflon was RCA<sup>[8]</sup> cleaned. The coating and curing procedures for THERMID given by the National Starch & Chemical Co. were strictly followed. On the top of the THERMID, two parallel 46 mm long stripes of aluminum with a 0.8 mm gap between them were deposited. They served as electrodes during the surface resistivity measurements. The sample as tested is schematically shown in Fig. 2-11.

### 2.3.2 Measurement method and Results

The sample as shown in Fig. 2-11 was used, to measure surface resistivity of THERMID. The current flux divergence at the terminals of the two strip electrodes can be neglected because of the large ratio of  $L/W$ , where  $L$  is the length of the strip electrode,  $W$  is the gap between the two electrodes. Once the leakage current flowing between the two strip electrodes,  $I$ , is measured, the surface resistivity  $\rho_s$  can be calculated from the applied voltage  $V$  using the following equation :

$$\rho_s = \frac{LV}{WI} \quad (2-2)$$

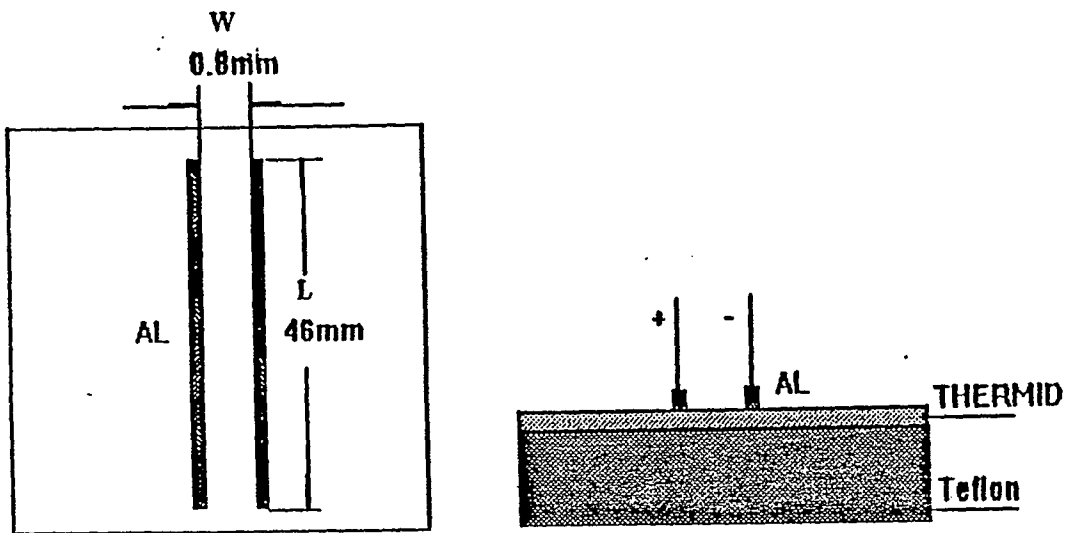


Fig. 2-11 Sample Schematic of surface resistivity measurement

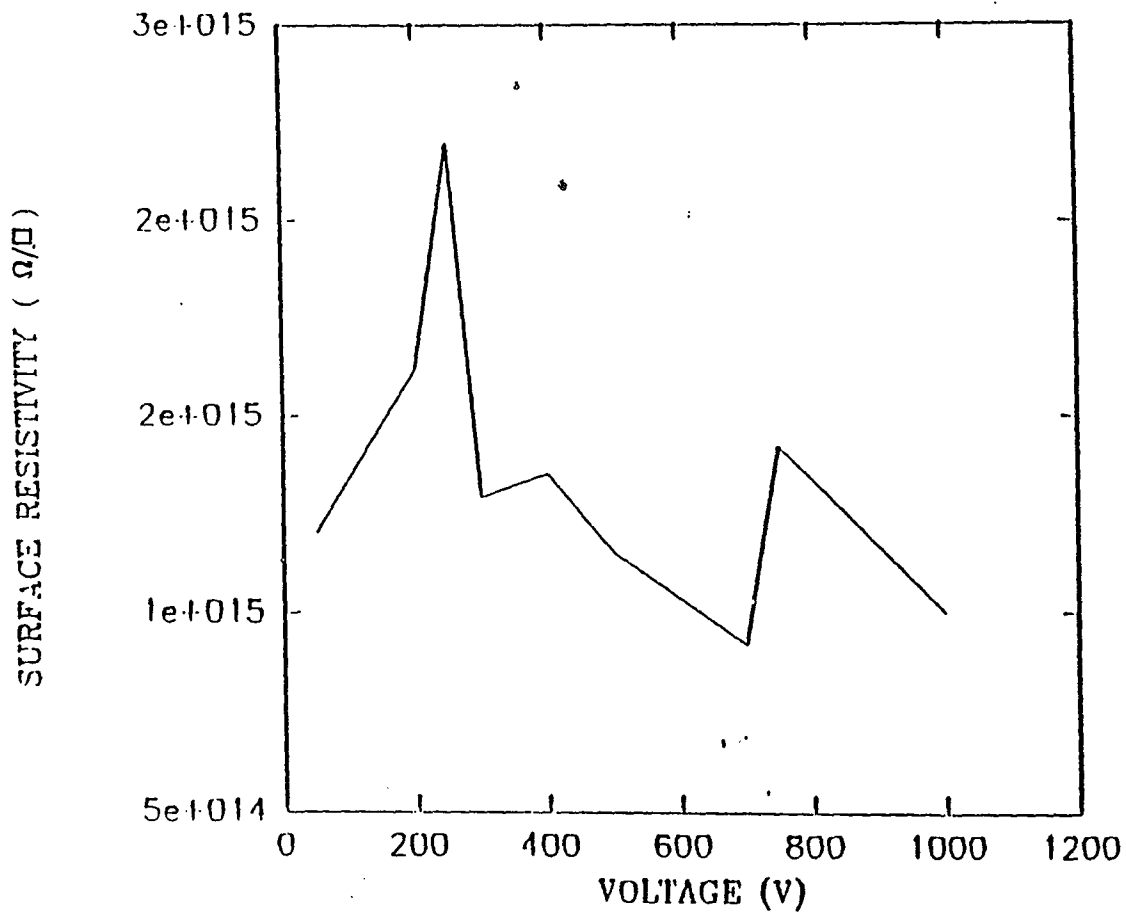


Fig. 2-12 Surface resistivity of THERMID at Room Temperature

Results of the measurement showed that the room temperature surface resistivity of THERMID is no less than  $1 \times 10^{15} \Omega/\square$ . ( See Fig. 2-12. )

## 2.4 Discussion

There are several probable causes that may render the measured bulk resistivity of the THERMID EL-5010 unreliable. But experiments showed that those causes can be ruled out as follows:

(1) Surface Leakage: While keeping the thickness of THERMID EL-5010 constant, different size of test spots were used. The data of the measurements were then scaled using equation 2-1. If surface leakage were the dominant mechanism responsible for the leakage, the leakage current should have been scaled with the circumference of the test spot, not the area of the spot as shown in table 2-1.

(2) Metal-THERMID EL-5010 Contact: While keeping the size of test spots constant, different thickness of THERMID EL-5010 thin film were used. The data of the measurements were then scaled using equation 2-1. If the metal-THERMID contact were the main mechanism determining the leakage current, the leakage current would not have scaled inversely with the thickness of the THERMID thin film as shown in table 2-1.

(3) Mobile Ion Motion: Following the theory of MOS capacitor structure, it was suggested that at room temperature, the mobile ions were basically bonded in the traps near the interface of THERMID and metal. They could not be moved to the interface of THERMID and silicon by the applied electrical field. The C-V measurements before and after temperature-bias stress, which is described in chapter 3, showed that this suggestion was true. Thus, the measurement error caused by the

mobile ions can be neglected too.

(4) Long Time to Reach Steady Leakage Current: The cause of the fairly long time needed to reach the steady leakage current, as shown in Fig 2-5, can be explained as follows. When a voltage is applied to a MIS capacitor, where polymer is used as dielectric, the current usually composes of charging current, absorption current, and leakage current. The absorption current is due to the dipoles and bonded ions in the polymer dielectric. Under the force of the applied electrical field, dipoles will be turned and bonded ions elasticly shifted. These will generate current. The absorption current can exist from seconds to minutes, depending upon different materials. That is why that although the time constant RC of the test circuit was estimated only several seconds, in our experiment it took 3 minutes for the current to reach its steady value - the bulk leakage current, which kept the same even if we waited for three more minutes as shown in fig.2-5.

Electrical conduction in organic materials may occur through the movement of either electrons or ions. Mechanisms which have been employed to explain the electrical conductivity of organic materials include<sup>[10]</sup>: ionic conduction, band-type conduction, hopping conduction, excitonic conduction, and tunnelling between metallic domains. Most common polymers have high resistivity since the electrons and ions are tightly bound in covalent bonds. Polar polymers have higher conductivity than non-polar polymers because of the electric dipole which is present<sup>[11]</sup>. The electrical properties of polymers depend more on an unbalance or asymmetry of dipoles than on the presence of polar groups<sup>[12]</sup>.

Fig.2-13 shows the chemical structure of both THERMID EL(electronic grade)-5010:

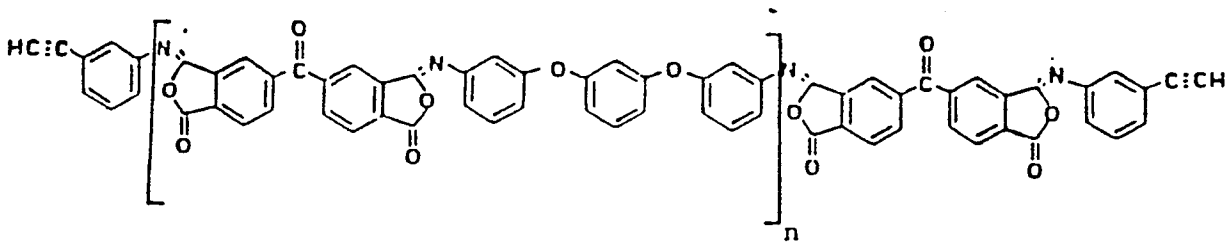


Fig. 2-13 Structure of THERMID EL-5010

THERMID at room temperature has very high resistivity since the electrons and ions in the THERMID are tightly bound in covalent bonds. Above a certain temperature, its resistivity begins to decrease because the temperature dependence of polyimide's resistivity is determined by its softening point<sup>[13]</sup>. When the temperature increases further, THERMID begins to decompose just as other polymers. The imide rings are destroyed, giving out CO gas and forming residues that contain NC. As there is a certain concentration of unsaturated free radicals in these residues, the electrical insulation property of THERMID becomes worse.

The breakdown in THERMID film can be either intrinsic or extrinsic. The intrinsic breakdown is caused by an electrical field in excess of its dielectric breakdown strength. The extrinsic breakdown is caused by an arc discharge, or electric spark, which normally takes place at points of defects, pinholes, and cracks in the dielectric film. At that time THERMID is decomposed and its resistivity sharply decreases as explained before. The 350 V/ $\mu$  breakdown voltage measured in our experiments is the intrinsic breakdown voltage of the THERMID thin film, whereas 180 V/ $\mu$  and 200 V/ $\mu$  breakdown voltages shown in table 2.1 are extrinsic breakdown voltages.

## Chapter 3 Fixed Charge and Mobile ion in the THERMID Layer

### 3.1 Test Principle

In order to obtain the parameters of fixed charge concentration and mobile ion concentration in THERMID layer, high frequency C-V characteristic measurement technique of MIS structure was used.

#### 3.1.1 MIS Structure Model

The MIS structure used in the experiment was shown in Fig. 3-1

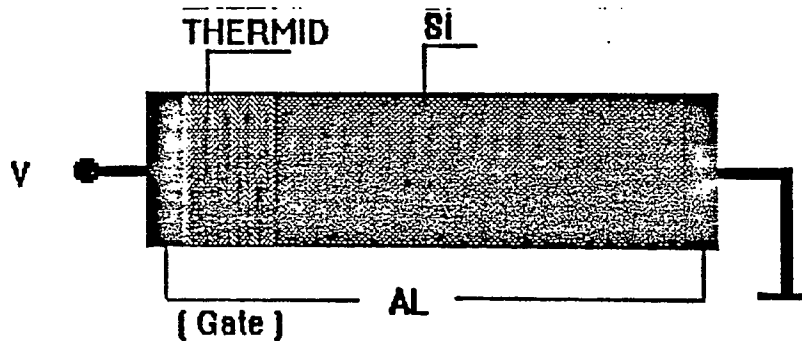


Fig. 3-1 MIS structure used in the experiment where THERMID served as an insulator layer

In depletion, weak inversion, and strong inversion regimes, the equivalent circuit of this MIS structure can be represented by Fig. 3-2<sup>[14]</sup>

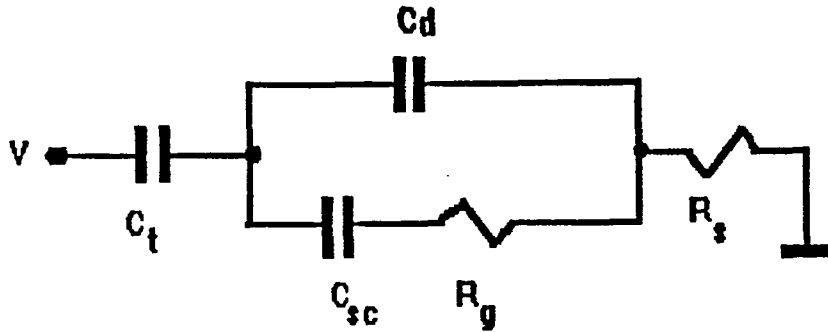


Fig. 3-2 Equivalent circuit of the MIS structure of Fig. 3-1

where

$$C_t = \frac{\epsilon_t S}{d_t}$$

$$C_d = \frac{\epsilon_s S}{d_d}$$

$C_t$  = insulator ( THERMID ) capacitance ( F or Coulombs/V )

$C_d$  = depletion layer capacitance of Si ( F )

$C_{sc}$  = capacitance related to the free carriers induced in the semiconductor by gate voltage ( F )

$S$  = gate area of MIS structure (cm<sup>2</sup>)

- $\epsilon_s$  = permittivity of silicon =  $8.854 \times 10^{-14} \times 11.8$  ( F/cm )  
 $\epsilon_t$  = permittivity of THERMID =  $8.854 \times 10^{-14} \times 3.0$  ( F/cm )  
 $d_t$  = thickness of THERMID thin film ( cm )  
 $d_d$  = width of depletion layer ( cm )  
 $R_s$  = substrate resistance (  $\Omega$  )  
 $R_g$  = differential resistance (  $\Omega$  )

$$R_g = \left( \frac{2N_d V_s}{\epsilon_s q} \right)^{\frac{1}{2}} (\tau_g / (N_i S))$$

$N_d$  = semiconductor bulk doping concentration (  $\text{cm}^{-3}$  )

$V_s$  = surface potential, measured with respect to the bulk of semiconductor substrate far from the interface ( V )

$\tau_g$  = effective generation time constant ( second )

$N_i$  = intrinsic carrier concentration of silicon =  $1.5 \times 10^{10}$  (  $\text{cm}^{-3}$  ) at 300°K

$q$  = fundamental electronic charge =  $1.6 \times 10^{-19}$  ( Coulombs or A x second )

The small-signal impedance of the equivalent circuit shown in Fig. 3-2 can be further presented as a series combination of a frequency-dependent equivalent circuit shown in Fig. 3-3<sup>[14]</sup>

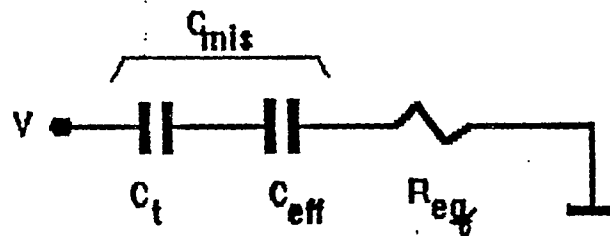


Fig. 3-3 Frequency-dependent equivalent circuit of Fig. 3-2

where 
$$C_{mis} = \frac{C_t C_{eff}}{(C_t + C_{eff})} \quad (3-1)$$

$$C_{eff} = \frac{(C_{sc} + C_d)^2 + \omega^2 C_d^2 C_{sc}^2 R_g^2}{C_{sc} + C_d + \omega^2 C_d C_{sc}^2 R_g^2} \quad (3-2)$$

$$R_{eq} = R_s + \frac{C_{sc}^2 R_g}{(C_{sc} + C_d)^2 + \omega^2 C_d^2 C_{sc}^2 R_g^2} \quad (3-3)$$

$\omega = 2 \pi f$ ,  $f =$  frequency of signal

In a limiting case of  $\omega \Rightarrow \infty$ , eq.(3-1), to (3-3) become

$$C_{eff} = C_d \quad (3-4)$$

$$R_{eq} = R_s \quad (3-5)$$

$$C_{mis} = \frac{C_t C_d}{C_t + C_d} \quad (3-6)$$

So under high frequency, and in depletion, weak inversion and strong inversion regions, the MIS structure can be presented as equivalent circuit shown in Fig. 3-4

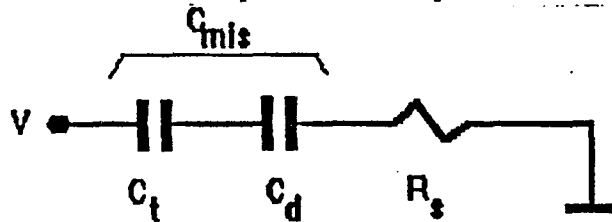


Fig. 3-4 Equivalent circuit of MIS under high frequency

### 3.1.2 Principle of High Frequency C-V Characteristic Measurement

The set-up of the high frequency C-V measurement is illustrated schematically in the block diagram shown in Fig. 3-5

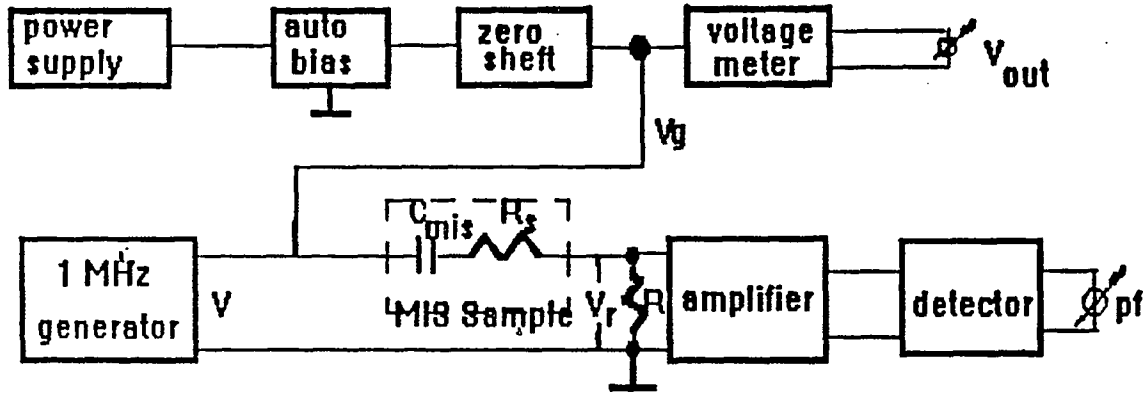


Fig.3-5 Principle block diagram of high frequency C-V measurement

where the 1 MHz signal generator is a low impedance, high frequency sine wave generator. Its output voltage,  $V$ , can be basically kept constant while the MIS structure capacitance under measurement is varying.  $R$  is a  $50 \Omega$  resistor put at the input port of amplifier. The magnitude of the a-c voltage drop across this resistor,  $V_r$ , can be represented as

$$V_r = \frac{V R}{((R+R_s)^2 + (1/(\omega C_{mis}))^2)^{1/2}} \quad (3-7)$$

where  $\omega = 2 \pi f$                        $f = 1 \text{ MHz}$

By choosing the value of  $S$  and  $d_t$  in eq.  $C_t = \epsilon_t S/d_t$ , we can ensure the capacitance of the MIS structure,  $C_{mis}$ , to be less than 200 pf. Thus we have

$$\left( \frac{1}{\omega C_{mis}} \right)_{min} = \frac{1}{2\pi \times 10^6 \times 200 \times 10^{-12}} \approx 800\Omega$$

Because  $R_s$  is usually less than  $30 \Omega$  ( if only the substrate resistivity of Si wafer is no more than  $10 \Omega\text{-cm}$  and the gate diameter of the MIS structure is no less than 1 mm), so during C-V measurement we always have

$$\frac{1}{\omega C_{mis}} \gg R + R_s$$

Thus eq. (3-7) becomes

$$V_r = V\omega C_{mis}R \tag{3-8}$$

because  $V$ ,  $\omega$ , and  $R$  are constants , so

$$V_r \propto C_{mis}$$

This means that  $V_r$  directly reflects the capacitance of MIS structure.

The auto bias generator shown in Fig.3-5 is used to produce a series of D.C. biases, which serve as the gate voltage  $V_g$  of MIS structure, to make changes of the

MIS structure capacitance so that a C-V plot can be produced.

### 3.1.3 Measurement of flatband capacitance and flatband voltage

In order to calculate the fixed charge concentration in the THERMID layer and subsequently the mobile ion concentration, we first need to calculate the flatband capacitance and voltage. Under the flat-band condition, we have<sup>[14][15]</sup>

$$C_{fb} = \frac{C_i C_{so}}{C_i + C_{so}} \quad (3-9)$$

$$C_{so} = \epsilon_s S / L_{dp}$$

$$L_{dp} = [ \epsilon_s K T / (q^2 N_d) ]^{1/2}$$

where  $C_{fb}$  = flatband capacitance ( F )

$C_{so}$  = Debye capacitance ( F )

$L_{dp}$  = Debye length ( cm )

$K$  = Boltzman constant (  $1.38 \times 10^{-23}$  Joules/ $^{\circ}K$  )

$T$  = temperature ( $^{\circ}K$  )

During C-V measurement, the maximum MIS structure capacitance can be obtained at accumulation region (where  $C_d \Rightarrow \infty$  ). From eq.(3-6) we find

$$C_{mis(max)} = C_i$$

thus eq.(3-9) becomes

$$C_{fb} = \frac{C_{max}C_{so}}{C_{max}+C_{so}} \quad (3-10)$$

During C-V measurement the flatband voltage is obtained as the voltage at which the observed (measured) capacitance is equal to the theoretical flatband capacitance calculated by eq. (3-10)

### 3.2 Measurement Method

#### 3.2.1 Measurement Method — If There Is No Mobile Charge in THERMID at Room Temperature

As soon as the flatband voltage is obtained, the fixed charge concentration in the THERMID layer can be calculated by eq. (3-11)

$$N_f = Q_f/q = -(C_i/q)(V_{fb} - \phi_{ms}) = -(\epsilon_i/(qd_i))(V_{fb} - \phi_{ms}) \quad (3-11)$$

$$\phi_{ms} = \phi_m - (X_{si} + (E_g/(2q)) - \phi_n)$$

$$\phi_n = (KT/q) \ln(N_d/N_i)$$

where  $\phi_{ms}$  = Metal - Semiconductor work function difference ( V )

$\phi_m$  = Fermi level of metal ( V )

$X_{si}$  = electron affinity of silicon ( V )

$\phi_n$  = surface potential of n-type substrate ( V )

$E_g$  = forbidden band width of Si ( eV )

In order to measure mobile ion concentration, temperature-bias stresses should be done during C-V measurement. If there is no mobile charge in the THERMID layer at room temperature, only positive temperature-bias stresses are needed. The following procedures are positive temperature-bias stresses:

(1) temperature : 200°C

    bias on gate : 20 V

    time : 20 min.

The purpose of this procedure is to drive any mobile ion out of THERMID to the Si/THERMID interface.

(2) cool to room temperature while keeping the 20 V bias on gate and do C-V measurement to find flatband voltage after the positive temperature-bias stresses.

The mobile ion concentration in the insulator layer,  $N_m$ , can be obtained from the change of the flatband voltage after the temperature-bias stresses :

$$N_m = Q_m/q = - (C_i/q)\Delta V_{fb} = - (\epsilon_i/q) (\Delta V_{fb}/d_i) \quad (3-12)$$

$$\Delta V_{fb} = V'_{fb} - V_{fb}$$

where  $V_{fb}$  = flatband voltage at room temperature before positive temp.-bias stress

$V'_{fb}$  = flatband voltage at room temperature after positive temp.-bias stress

### 3.2.2 Measurement Method — If There are Mobile Charges in THERMID at Room Temperature

If there are mobile charges in the THERMID layer at room temperature, much more strict measurement procedures will be needed. The temperature-bias stresses should follow steps shown in table 3-1:<sup>[16]</sup>

<u>Step</u>	<u>Condition</u>	<u>Function</u>	<u>Charge at the interface of THERMID - Si</u>
1	$V_g = 0$ $T = 250^\circ\text{C}$	exciting the ions in traps	
2	$V_g = +20\text{V}$ $T = 25^\circ\text{C}$	drive room temp. mobile "+" charge to interface of TH.-Si	fixed charge + room temp. mobile charge
3	$V_g = +20\text{V}$ $T = 200^\circ\text{C}$	drive sodium ion to interface of THERMID-Si	fixed charge + room temp. mobile charge + Sod. ion
4	$V_g = -20\text{V}$ $T = 25^\circ\text{C}$	draw back room temp. mobile "+" charge to interface of Met.-TH.	fixed charge + sodium ion
5	$V_g = -20\text{V}$ $T = 200^\circ\text{C}$	draw back sodium ion to inter- face of Metal-THERMID	fixed charge

Table 3-1 Temperature-bias Procedures if Mobile ion existing in the THERMID at Room Temperature

The fixed charge concentration can be obtained by step 5:

$$N_f = - (\epsilon_t/q)((V_{fb}^{(5)} - \phi_{ms})/d_t) \quad (3-13)$$

The sodium-ion concentration can be obtained by step 2, step 3 or by step 4, step5:

$$N_m = (\epsilon_t/q)((V_{fb}^{(2)} - V_{fb}^{(3)})/d_t) = (\epsilon_t/q)((V_{fb}^{(5)} - V_{fb}^{(4)})/d_t) \quad (3-14)$$

The room temperature mobile charge can be obtained by step 3, step4:

$$N_m = (\epsilon_t/q)((V_{fb}^{(4)} - V_{fb}^{(3)})/d_t) \quad (3-15)$$

### 3.3 Sample Preparation

#### 3.3.1 Parameter selection of the MIS structure

In order to obtain useful C-V measurement data, the MIS structure sample should be carefully prepared. Among all parameters of the sample, most important ones are doping concentration of the silicon wafer and the thickness of the insulator (THERMID). From the above discussion, during C-V measurement the maximum capacitance will appear in accumulation region and is no other than the THERMID capacitance :

$$C_{max} = C_t = \epsilon_t S/d_t \quad (3-16)$$

The minimum capacitance will appear in strong inversion region which can be obtained from eq.(3-6):

$$C_{min} = (C_t C_{inv}) / (C_t + C_{inv}) = (C_{max} C_{inv}) / (C_{max} + C_{inv}) \quad (3-17)$$

$$C_{inv} = (\epsilon_s S) / d_{inv} \quad (3-18)$$

$$\begin{aligned} d_{inv} &= 2 [ \epsilon_s \phi_b / (q N_d) ]^{1/2} = 2 [ \epsilon_s ((KT/q) \ln(N_d/N_i)) / (q N_d) ]^{1/2} \\ &= 2 [ ((\epsilon_s KT) / (q^2 N_d)) \ln(N_d/N_i) ]^{1/2} \end{aligned} \quad (3-19)$$

where  $C_{inv}$  = capacitance of strong inversion region ( F )

$d_{inv}$  = depletion layer width of strong inversion ( cm )

$\phi_b$  = difference between the Fermi level and intrinsic Fermi level ( V )

from eq. (3-16) - (3-19), we can obtain the ratio of  $C_{min}$  and  $C_{max}$

$$\begin{aligned} C_{min}/C_{max} &= [1 + (C_{max}/C_{inv})]^{-1} \\ &= \{1 + (2\epsilon_t / (\epsilon_s d_t)) [((\epsilon_s KT) / (q^2 N_d)) \ln(N_d/N_i)]^{1/2}\}^{-1} \end{aligned} \quad (3-20)$$

Choosing lightly doped N-type silicon wafer with a resistivity of 2-5 ohm-cm (corresponding to bulk doping concentration of  $2 \times 10^{15}$  -  $9 \times 10^{14}/\text{cm}^2$ ) and 0.8  $\mu$  thickness of THERMID layer, we can expect a reasonable ratio of  $C_{min}/C_{max}$  in the C-V curve by using eq. (3-20) as shown in table 3-2

$\rho$ (ohm-cm)	$d_t$ ( $\mu\text{m}$ )	$C_{min}/C_{max}$
2	0.8	0.833
3	0.8	0.813
4	0.8	0.784
5	0.8	0.776

Table 3-2 Ratio of  $C_{min}/C_{max}$  estimated by eq.(3-20)

### 3.3.2 Sample Preparation

According to section 3.3.1, for our C-V measurement, lightly doped N-type wafers with a resistivity of 4-5 ohm-cm were used. All wafers were cleaned by using RCA<sup>[8]</sup> technique followed by a HF dip and thorough rinsing with deionized water. All microelectronic processing operations were performed in a class 100 clean room. Just before THERMID EL-5010 formulation which was prepared by National Starch & Chemical Co. was coated on the wafers, these wafers were all treated in HF liquid to get off any SiO<sub>2</sub> thin films that were formed on them by oxidation. The Si wafers were then coated with THERMID EL-5010 strictly following the technology given by National Starch & Chemical Co. to the thickness of 0.72-0.76  $\mu\text{m}$ . The cure procedures followed were 180°C(30 min.), 300°C(60 min), and 400°C(15 min.). After that the backs of the wafers were sanded to get off the SiO<sub>2</sub> and then deposited a thin film of aluminum. On top of the THERMID film, aluminum spots with dimensions of 1mm - 3mm were deposited. The final MIS structure sample for C-V measurement was schematically shown in Fig.3-6.

### 3.4 Test Results

The actual C-V measurements were done by using C-V Plotter manufactured by the Micromanipulator Co., Inc. Tests before and after positive temperature-bias stresses, which are described in section 3.2.1, were performed separately. The constants needed by "C-V Measurement Analysis Programs" are shown in Table 3.3. The results of the C-V measurement before positive temperature-bias stresses are shown in Fig.3.7 and table 3.4. The results after positive temperature-bias stresses are shown in Fig.3.8 and Table 3.5. By using eq.3.11 and eq.3.12 we found that the fixed charge in the THERMID EL-5010 thin film is negative and has a concentration of around  $10^{11} \text{ cm}^{-2}$ . The mobile ion concentration in the THERMID EL-5010 thin film is  $1.12 \times 10^{11} \text{ cm}^{-2}$ .

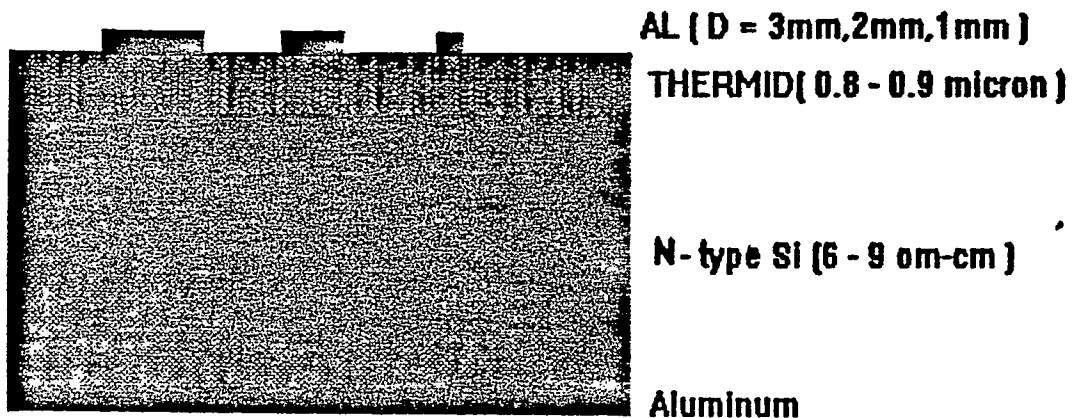


Fig. 3-6 Sample Schematic for C-V Measurement of MIS  
 THERMID was used as Insulator Dielectric

THERMID PERMITTIVITY .....	2.800
SEMICOND PERMITTIVITY .....	11.70
GATE WORK FUNCTION (V) .....	4.200
WORK FUNCTION DIFF (V) .....	-.3000
ENERGY BAND GAP (V) .....	1.120
ELECTRON AFFINITY (V) .....	3.780
SQRT OF $N_c \cdot N_v$ (CM-3) .....	3.050E15
INTRINSIC CONC (CM-3) .....	1.500E10

Table 3.3 Constants Needed by "C-V Measurement Analysis Programs"  
 for the C-V Measurement of MIS Where THERMID Was Used  
 as Insulator Dielectric (at 300°)

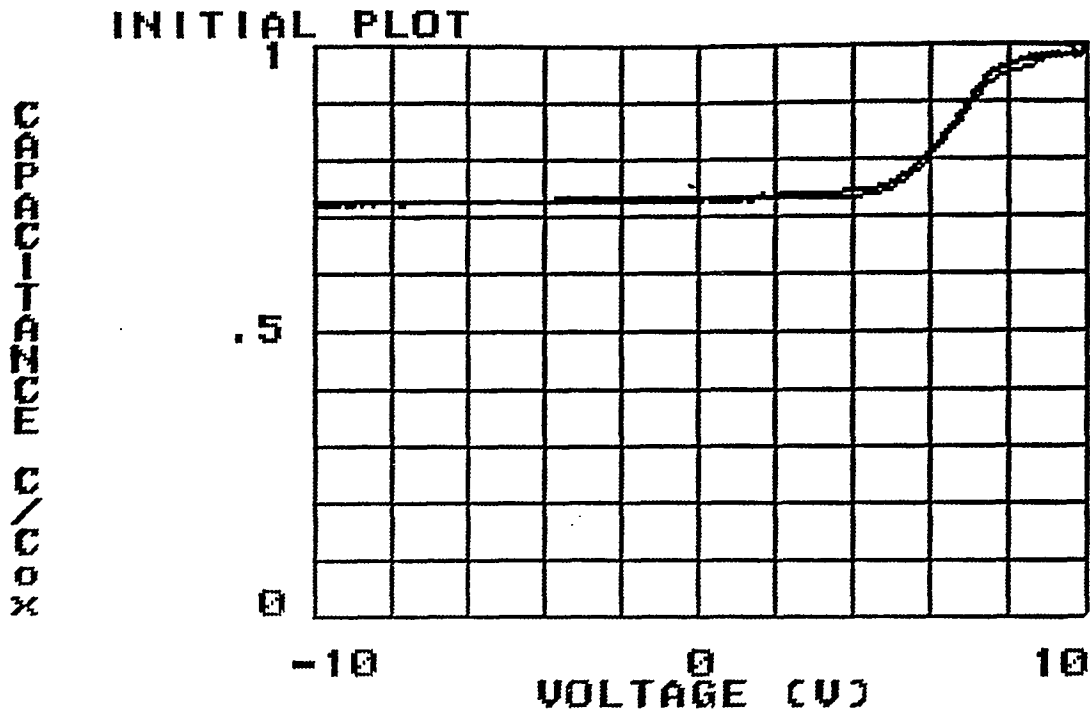


Fig. 3.7 C-V Curve of the MIS Before Positive Temperature-bias Stress,  
THERMID Was Used as Insulator Dielectric

```

CV PLOT
WAFER ID      : A3
DATE          : 4/10/91
TIME          : 11:41:46
TYPE          : N
MODE          : CAP
CMAX          : 101.4 PF
RATIO         : .7237
CFB           : 96.08 PF
AREA          : 3.065E-2 SQ CM
TTHERMID     : 7.495E3 A
VFB [1]      : 9.518 VOLTS
Nfixed       : -1.932E11 CM-2
VT           : -7.075 VOLTS
  
```

Table 3.4 Data of C-V Measurement Before Positive  
Temperature-bias Stress

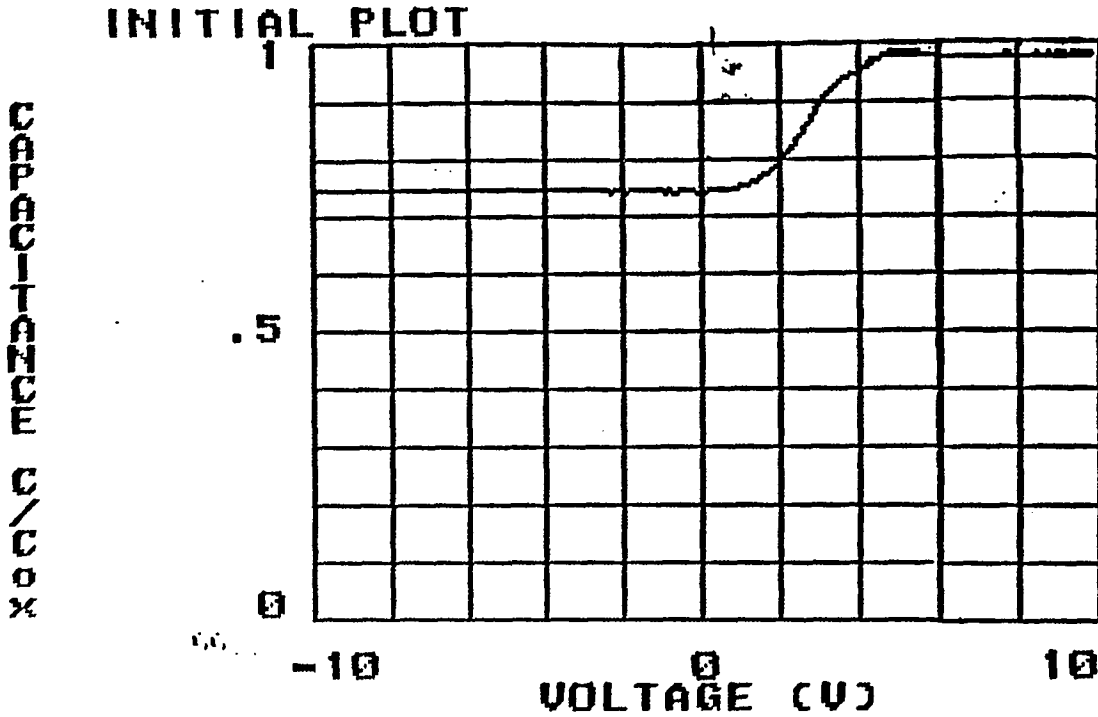


Fig. 3.8 C-V Curve of the MIS After Positive Temperature-bias Stress,  
THERMID Was Used as Insulator Dielectric

```

CV PLOT
WAFER ID      : A3
DATE          : 4/10/91
TIME         : 12:45:09
TYPE         : N
MODE         : CAP
CMAX        : 102.1 PF
RATIO       : .7235
CFB         : 95.73 PF
AREA        : 3.065E-2 SQ CM
TTHERMID    : 7.495E3 A
VFB [2]     : 4.095 VOLTS
Nfixed      : -8.112E10 CM-2
VT          : 0.5 VOLTS

```

Table 3.5 Data of C-V Measurement After Positive  
Temperature-bias Stress

### 3.5 Discussion

The fixed charge concentration and mobile ion concentration in the THERMID thin film are two very important parameters. The fact that there are  $10^{11}$   $\text{cm}^{-2}$  negative fixed charges in the THERMID thin film is very interesting and significant. The cause of these negative fixed charges is perhaps the weak bond of the H-C\* (C\* means triple carbon bond) end of the THERMID molecular chain (which is shown in Fig.2-13). Because of the weak bond of the H-C\* end, hydrogen atom tends to escape by any activation energy, leaving a radical at the end of the THERMID molecule. The molecular chain is much bigger and more difficult to move than the  $\text{H}^+$ . As a result, a certain concentration of negative fixed charge is formed in the THERMID thin film.

We didn't expect the data of the mobile ion concentration obtained from our experiment to be very accurate. This is because the shift in flatband voltage may have one or more possible causes listed as follows: (1) Mobile ions, particularly sodium in THERMID; (2) Electrons or holes injected into the THERMID by the application of excessive voltage during the temperature-bias stresses; (3) Mobile impurities other than sodium; (4) Changes in measurement conditions, for example: the back-side ohmic and capacitative contact to the wafer, moisture on the surface. But these data certainly provide us with some significant information relevant to the production technology of THERMID. They are also very important to those who want to apply THERMID to HDI and MCM's technology.

## Chapter 4 Far-Infrared Absorption Properties of THERMID

### 4.1 Test Principle

In the far-infrared spectral region, one of the most useful methods to observe all the spectral details is to observe the interferogram of the spectral elements produced in a lamellar grating spectrometer. This interferogram contains all wavelengths (spectral elements) incident onto the spectrometer. But, since all the spectral elements are "mixed up", this interferogram cannot be used directly to obtain the spectral details. However, a Fourier transformation of the interferogram can be used to untangle the spectral elements.

#### 4.1.1 Fourier Transform spectroscopy<sup>[18][17]</sup>

Fourier transform spectroscopy applied to the millimeter wavelength region may provide continuous spectra desirable for the study of material properties over several octaves of the spectrum. The output intensity of the lamellar grating spectrometer for monochromatic light is:

$$J(Y) = 2 G_{\nu} [1 + \cos(2\pi\nu Y)] \quad (4-1)$$

where  $J(Y)$  is the output intensity of the lamellar grating spectrometer, which can

be obtained experimentally.

$Y$  = the optical path difference between the two sets of reflectors of the

lamellar grating  $Y = 2 (X_2 - X_1)$  ( in cm)

$\nu$  = the wave number ( in  $\text{cm}^{-1}$ )

$\nu = 1/\lambda$  ,  $\lambda$  = wavelength

$G_\nu$  = the intensity of the wave with wave number  $\nu$

For polychromatic light, we have the superposition of all the intensities of all spectral elements:

$$J(Y) = \sum_{\nu(i)=\nu(1)}^{\nu(n)} 2G_{\nu i} [1 + \cos(2\pi\nu_i Y)] \quad (4-2)$$

for the case of a continuous distribution of wave numbers

$$J(Y) = 2 \int_0^\infty G(\nu) [1 + \cos(2\pi\nu Y)] d\nu \quad (4-3)$$

for the specific case where  $Y = 0$

$$J(0) = 4 \int_0^\infty G(\nu) d\nu \quad (4-4)$$

We assume that  $G(\nu)$  is symmetric around  $\nu = 0$ , that is ,  $G(\nu) = G(-\nu)$

$$J(0) = 4 \int_0^\infty G(\nu) d\nu = 2 \int_{-\infty}^\infty G(\nu) d\nu \quad (4-5)$$

From eq. (4-3)

$$J(Y) = 2 \int_0^{\infty} G(\nu) d\nu + 2 \int_0^{\infty} G(\nu) \left( \frac{e^{i2\pi\nu y} + e^{-i2\pi\nu y}}{2} \right) d\nu \quad (4-6)$$

using eq.(4-4) and (4-5) in eq.(4-6) and since  $G(\nu) = G(-\nu)$ , we have:

$$J(Y) = \frac{1}{2} J(0) + \int_{-\infty}^{\infty} G(\nu) e^{i2\pi\nu y} d\nu \quad (4-7)$$

The interferogram function  $S(Y)$  is: ( See Fig. 4-1. )

$$S(Y) = J(Y) - \frac{1}{2} J(0) = \int_{-\infty}^{\infty} G(\nu) e^{i2\pi\nu y} d\nu \quad (4-8)$$

$S(Y) = J(Y) - \frac{1}{2} J(0)$  can be obtained experimentally by moving the movable set of reflectors of the lamellar grating spectrometer from  $Y = -L$  to  $Y = +L$ . Where  $L$  is the maximum optical path displacement between the two sets of reflectors of the lamellar grating spectrometer.

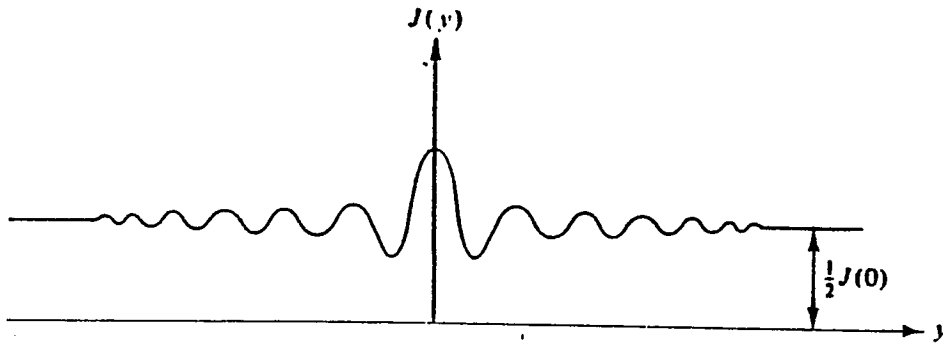


Fig. 4-1  $S(Y) = J(Y) - \frac{1}{2} J(0)$

To find  $G(\nu)$ , we observe that eq.4-8 can be identified as a Fourier integral and the inverse Fourier transformation integral is

$$G(\nu) = \int_{-\infty}^{\infty} S(Y) e^{-i2\pi\nu Y} dY \quad (4-9)$$

The integration is now over the space coordinate  $Y$ , and the wave number  $\nu$  appears as a parameter. In a computer sampling system, eq. (4-9) should be conveniently expressed in discrete form:

$$G(K\Delta\nu) = \sum_{J=-N/2}^{(N/2)-1} S(J\Delta Y) \exp[-i2\pi K\Delta\nu J\Delta Y] \quad (4-10)$$

In order to obtain the spectrum, it is only necessary to perform the calculation of eq.4-10.

The general method of obtaining a spectrum using a spectrometer is as follows:

- (1) Measure  $J(Y)$  by recording the signal versus the displacement of the movable set of reflectors, noting that  $Y = 2 X$  (where  $X$  is the displacement) [ The displacement is usually done in discrete steps ].
- (2) At zero path difference, experimentally determine  $J(0)$ .
- (3) Substitute  $[J(Y) - \frac{1}{2} J(0)] = S(Y)$  in eq. (4-10) and evaluate the integral for a chosen  $\nu$ .
- (4) Perform the integration of eq.(4-10) for each chosen  $\nu$ .
- (5) As a result of steps 1- 4, one has, with a multiplication constant, computed  $G(\nu)$  versus  $\nu$ , i.e., the spectrum.

#### 4.1.2 The Cooley - Turkey Algorithm<sup>[18]</sup>

The classical method of computing the discrete Fourier transform has been replaced for most purposes by the Cooley-Turkey algorithm. The main reason is the enormous saving in computation time. This algorithm extended the usefulness of Fourier spectroscopy into the near-infrared and visible wavenumbers regions. Cooley-Turkey algorithm leads naturally to calculating the Fourier transform for a set of  $\nu$  (wave number) that is given by

$$\{\nu_{max}/(N/2), \nu_{max}/[(N/2)-1], \dots, \nu_{max}\}$$

This is a set of  $N/2$  values of  $\nu$ , where

$N$  = sample point numbers of experimental interferogram which should be

$$N = 2^n \text{ (} n \text{ is integer)}$$

$\nu_{max}$  = the maximum wave number of the spectral range

With  $N/2$  spectral samples we have

$$\Delta\nu = \nu_{max}/(N/2) \tag{4-11}$$

According to the sampling theory, the maximum sampling path step that could be used is:

$$\Delta Y = 1/(2 \nu_{max}) \tag{4-12}$$

If we define  $L$  as the maximum optical path displacement from the origin during the

experiment , we have

$$(N/2) \Delta Y = L \quad (4-13)$$

Substituting (4-12) (4-13) into (4-11), we have

$$\Delta \nu = \frac{1}{2L} \quad (4-14)$$

and by (4-12) x (4-11), we have

$$\Delta \nu \Delta Y = \frac{1}{N} \quad (4-15)$$

Substitute (4-15) into (4-10)

$$G(K\Delta \nu) = \sum_{J=-N/2}^{(N/2)-1} S(J\Delta Y) \exp(-i2\pi KJ/N) \quad (4-16)$$

Now denote  $G(K\Delta \nu)$  by  $G(K)$ ,  $S(J\Delta Y)$  by  $S(J)$ , eq. (4-16) becomes

$$G(K) = \sum_{J=-N/2}^{(N/2)-1} S(J) \exp(-i2\pi KJ/N) \quad (4-17a)$$

or

$$G(K) = \sum_{J=0}^{(N/2)-1} S(J) \exp(-i2\pi KJ/N) + \sum_{J=-N/2}^{-1} S(j) \exp(-i2\pi KJ/N) \quad (4-17b)$$

It is convenient to eliminate negative indexes, which can be done because of the periodicity of  $\exp(-i2\pi KJ/N)$ . We do this by relabeling the  $S(J)$  by adding  $N$  to the index of negative  $J$  and recombining the two sums. Thus we have:

$$G(K) = \sum_{J=0}^{N-1} S(J) \exp(-i2\pi KJ/N) \quad (4-18)$$

eq. (4-18) is the key equation used by Cooley-Turkey algorithm to calculate spectral elements.

The detail of Cooley-Turkey algorithm will not be discussed here.

## 4.2 Test System

A Fourier transform spectrometer using a 250 watt mercury lamp, a lamellar grating and a dip-stick He-cooled detector was set up under the instruction of Dr. K.D. Moller<sup>[19]</sup>. The interferogram measurement was under the control of an IBM 386 AT personal computer via a White Box A/D and RS232 Communication Unit.  $N=2^n$  ( $n$  is integer) points interferogram data obtained by the spectrometer were fed to the computer and then processed into a spectrum by using the Cooley-Turkey Fourier transform algorithm.

The Test System is shown in Fig. 4-2. The lamellar grating had a grating constant of 1.8 cm and the plates could be moved backward and forward 7.5 cm from

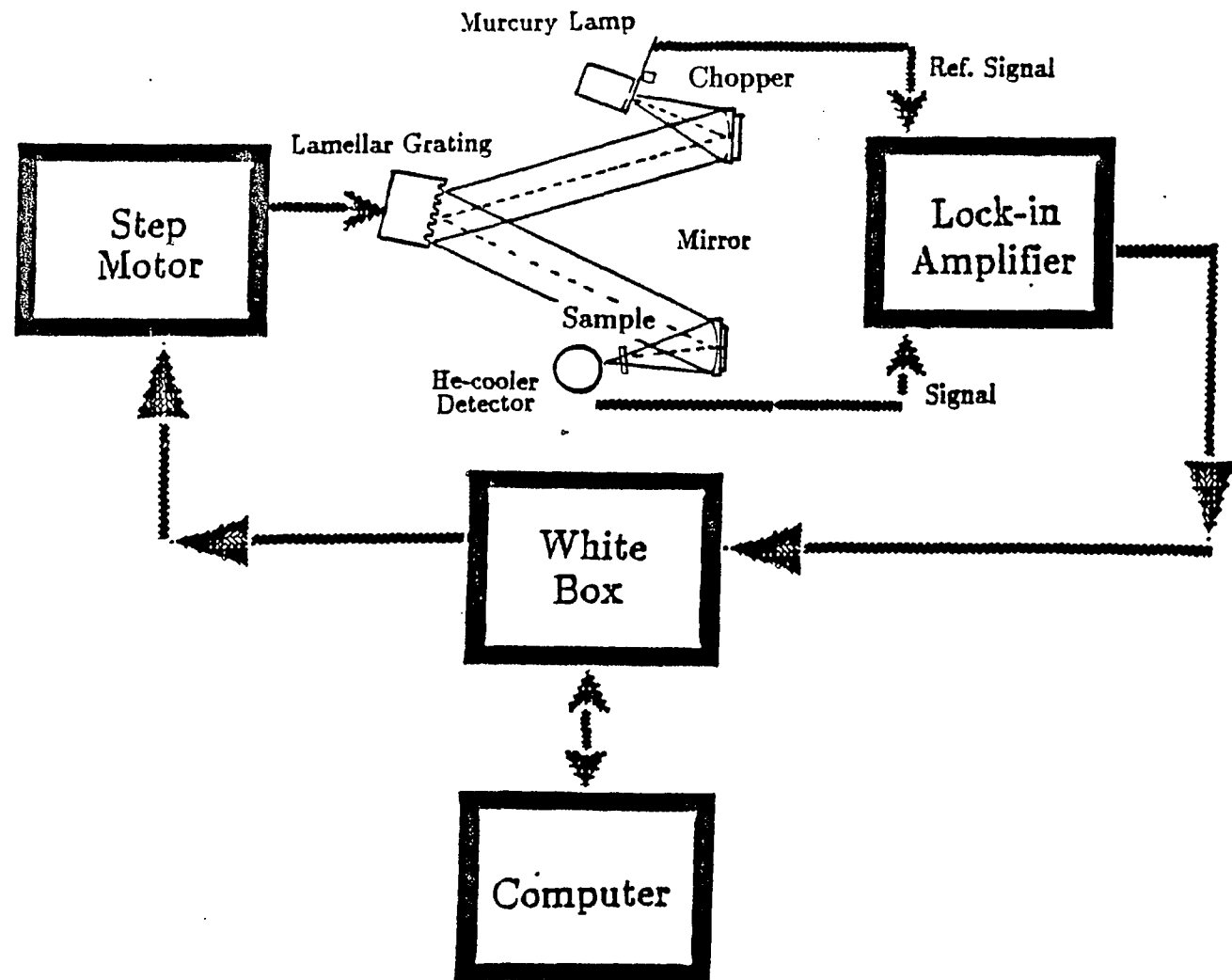


Fig. 4-2 Test System Schematic Diagram of Using Lamellar Grating Spectrometer to Measure Far-infrared Properties of THERMID

the zero position. The grating was used with the plates in horizontal position and the plates were made of aluminum. One stack of plates was fixed, the other was mounted on a carrier and could be moved with a stepping motor in such a way that each step of the motor resulted in a displacement of  $1.25\mu$ . The detector was a dipstick He-cooled bolometer manufactured by Dr. K. D. Moeller.

The system control, data processing and Cooley-Turkey Fourier Transform program were written in Quick Basic Language. ( See Appendix B. )

### 4.3 Measurement Method

In order to obtain an interferogram that is suitable for application of the Cooley-Turkey algorithm, the system was programmed to acquire 128 sample points by displacing the movable plate 128 times from negative position to positive position symmetrically across the zero position. Each time the plate was displaced by  $h=50\mu$  (corresponding to 40 steps of the motor), the optical path difference was increased by  $\Delta Y=2 \times 50\mu = 100\mu$  as shown in Fig. 4-3.

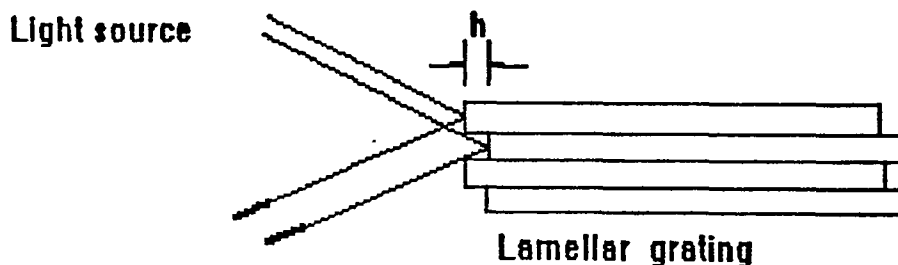


Fig. 4-3 Optical Path Difference in Experiment

The interferogram was a curve similar to the one shown in Fig. 4-4

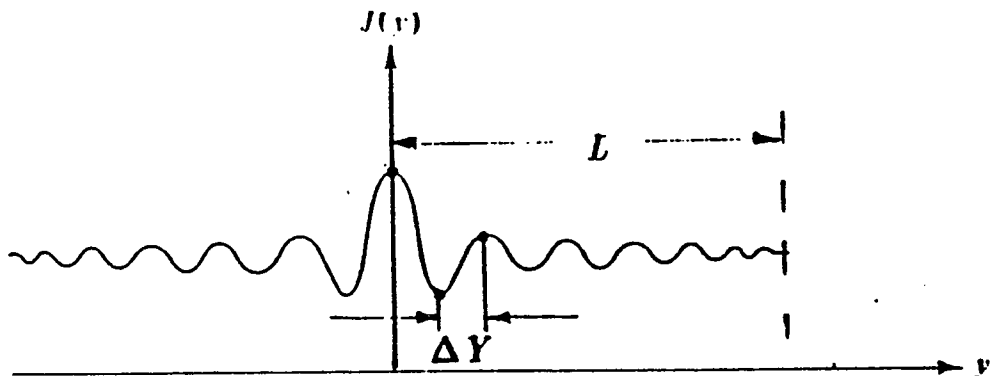


Fig. 4-4 Interferogram in Experiment

where the maximum optical path displacement  $L$  from origin (zero) position during the experiment was, according to eq.(4-13),  $L = 64 \times 100\mu = 6400\mu = 0.64$  cm. Substituting  $L$  into eq. (4-14), we have the resolution in wave numbers:

$$\Delta\nu = \frac{1}{2L} = \frac{1}{2 \times 0.64 \text{ cm}} = 0.78 \text{ cm}^{-1}$$

From eq.(4-11), the maximum wave number was

$$\nu_{max} = 64 \times \Delta\nu = 50 \text{ cm}^{-1}$$

This value is needed by the Cooley-Turkey algorithm to calculate the spectrum.

The sample used in the far-infrared absorption measurement of THERMID was provided by National Starch & Chemical Co. with a thickness of 3 mm.

#### 4.4 Test Results

The transmission spectrum of THERMID ,  $G_t(\nu)$ , in millimeter range is obtained as follows:

(1) measure the background interferogram (without THERMID sample in the optical path as shown in Fig.4-5) and calculate its correspond spectrum  $G_b(\nu)$  (as shown in Fig.4-7).

(2) measure the sample interferogram (with THERMID sample in the optical path as shown in Fig.4-6) and calculate its correspond spectrum  $G_s(\nu)$  (as shown in Fig.4-7).

where  $G_b(\nu)$  = spectrum without THERMID sample in optical path

$G_s(\nu)$  = spectrum with THERMID sample in optical path

(3) divide  $G_m(\nu)$  by  $G_b(\nu)$ , we have

$$G_t(\nu) = G_m(\nu)/G_b(\nu) \quad (4-19)$$

The corresponding transmission spectrum is shown in Fig.4-8. The data for Fig.4-7 and Fig.4-8 are shown in table 4-1.

We like to note that the absorption in the air and in the water vapor present in the air has been disregarded in this study.

The transmission spectrum II of the same THERMID sample shown in Fig.4-9 was obtained at Brookhaven National Laboratory. The source of the far infrared radiation in that experiment was the synchrotron. The spectrometer was a Nicolet Michelson scanning spectrometer and the detector was a pumped He-cooled

detector with  $10^{-14}$  NEP.

From Fig.4-8 and Fig.4-9 we found that the data obtained from the two systems match very well and have a smooth transfer.

Fig.4-8 and Fig.4-9 gave us a complete information about the transmission spectrum of the THERMID sample in the range of 1 - 60  $\text{cm}^{-1}$ .

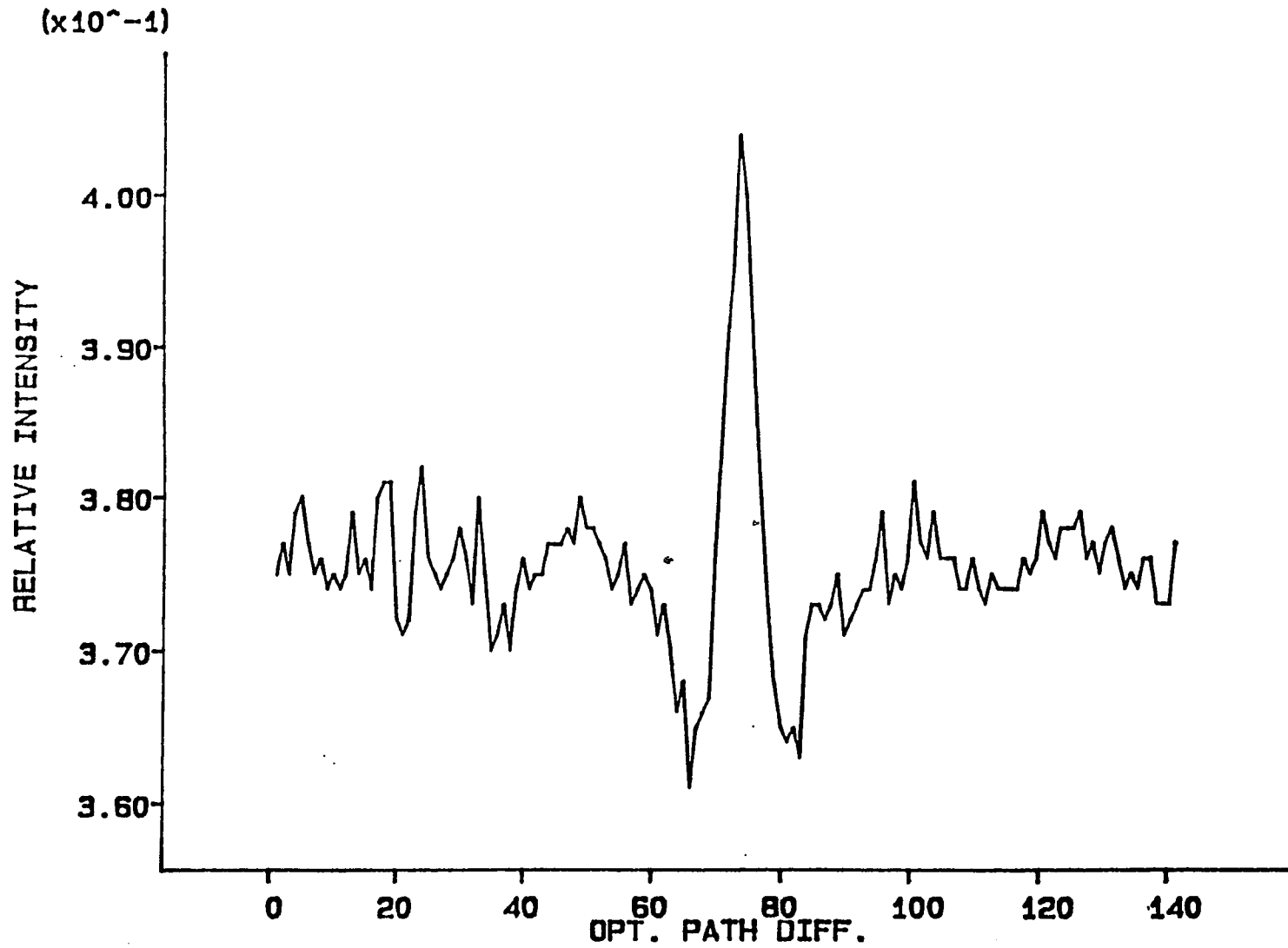


Fig. 4-5 The Interferogram of Background (Without THERMID in Optical Path)

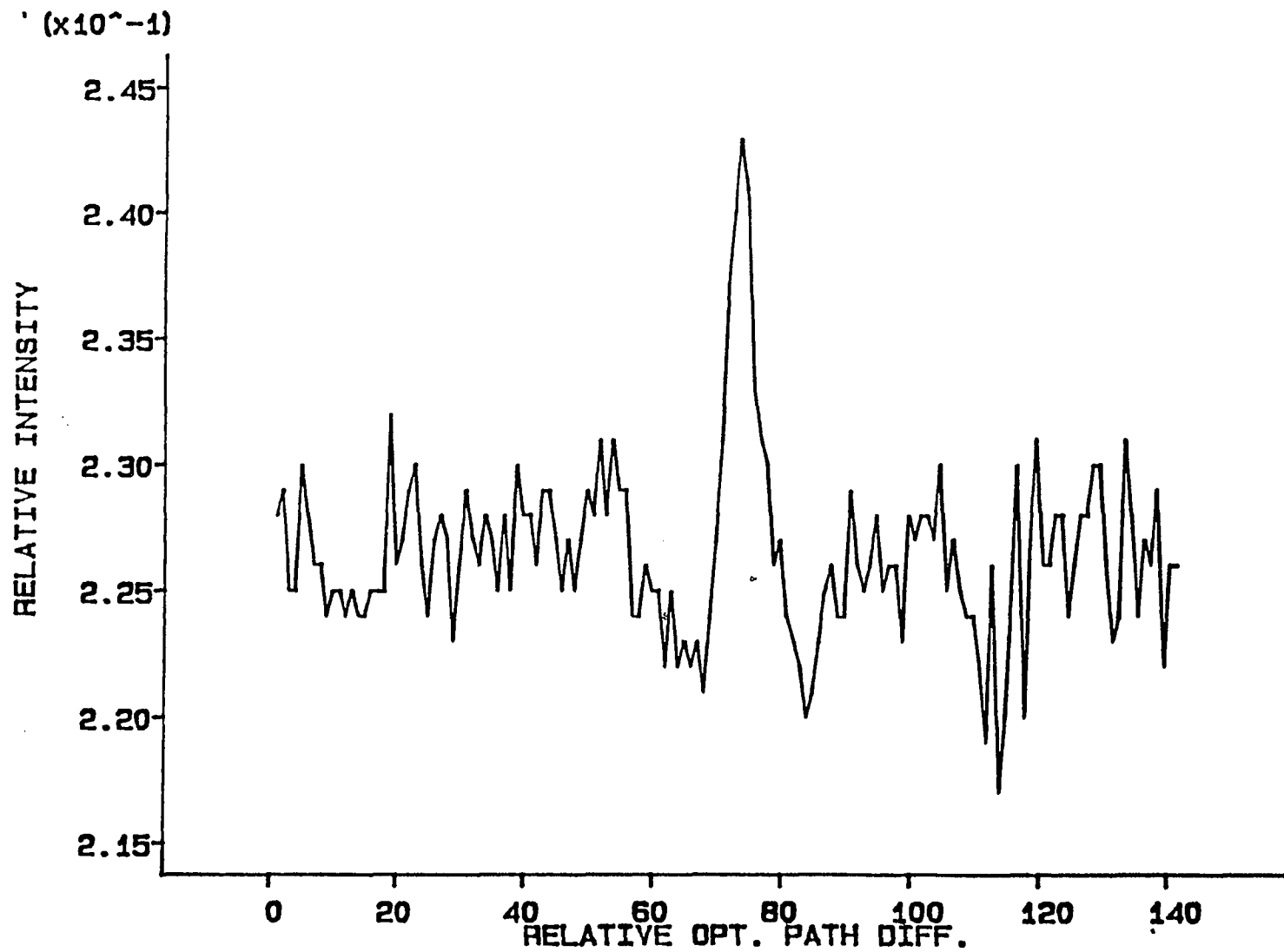


Fig. 4-6 The Mixed Interferogram (With THERMID in Optical Path)

# POLYIMIDE, about 3mm thick

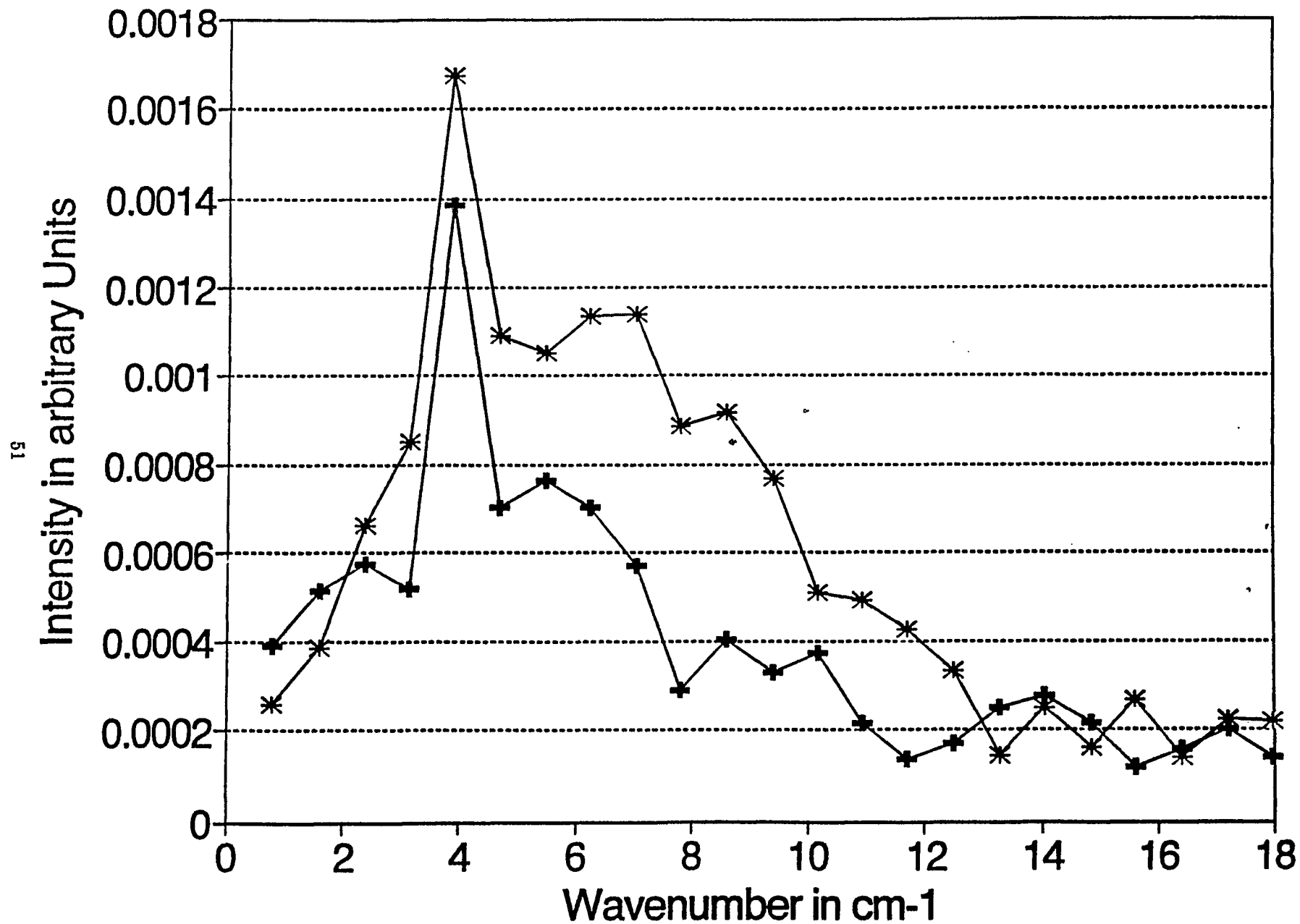


Fig. 4-7 Spectrum Obtained in Experiment:

\* — Without THERMID in the optical path

■ — With THERMID in the optical path

# POLYIMIDE, about 3mm thick

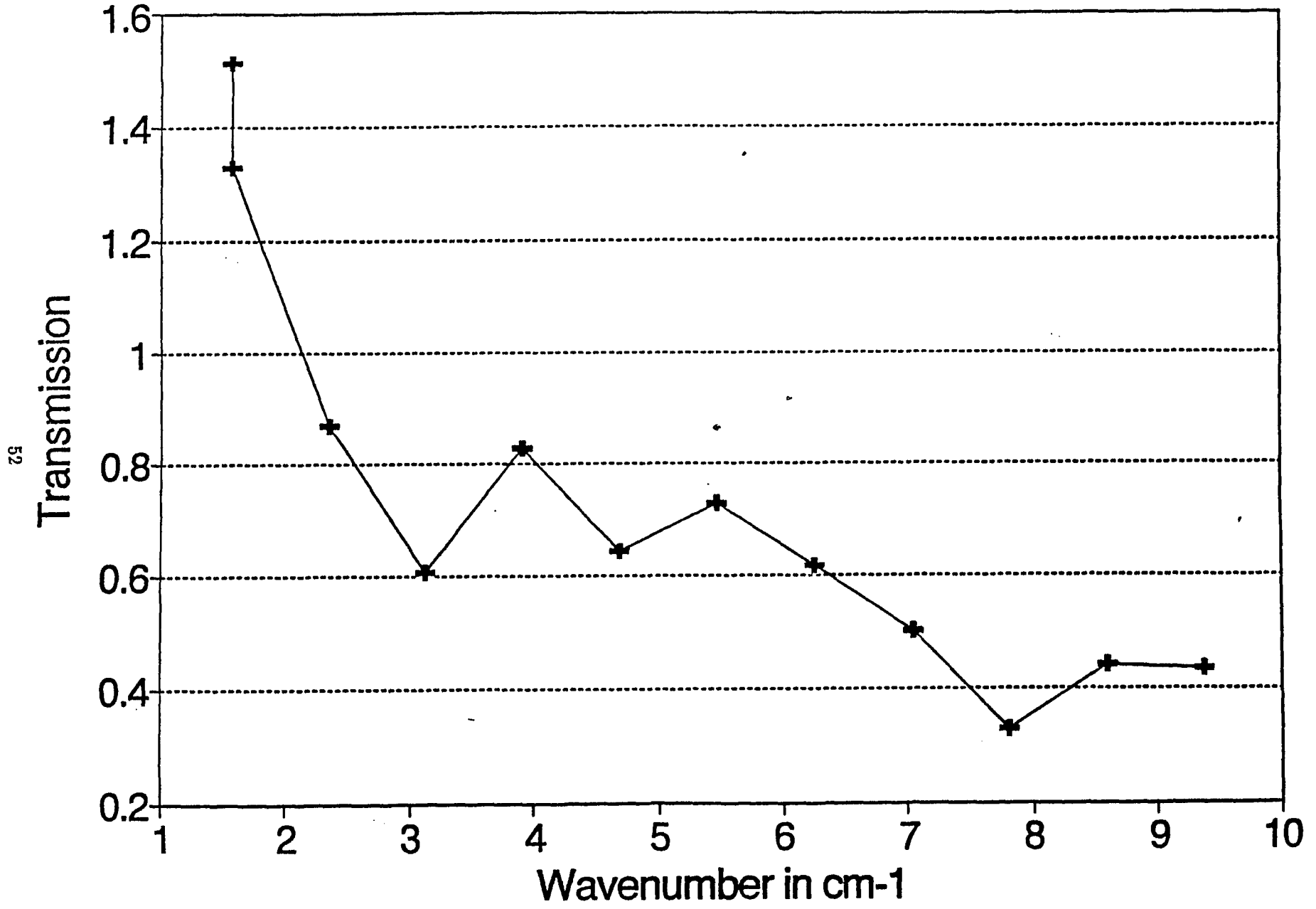


Fig. 4-8 THERMID Transmission Spectrum I

# POLYIMIDE, about 3mm thick

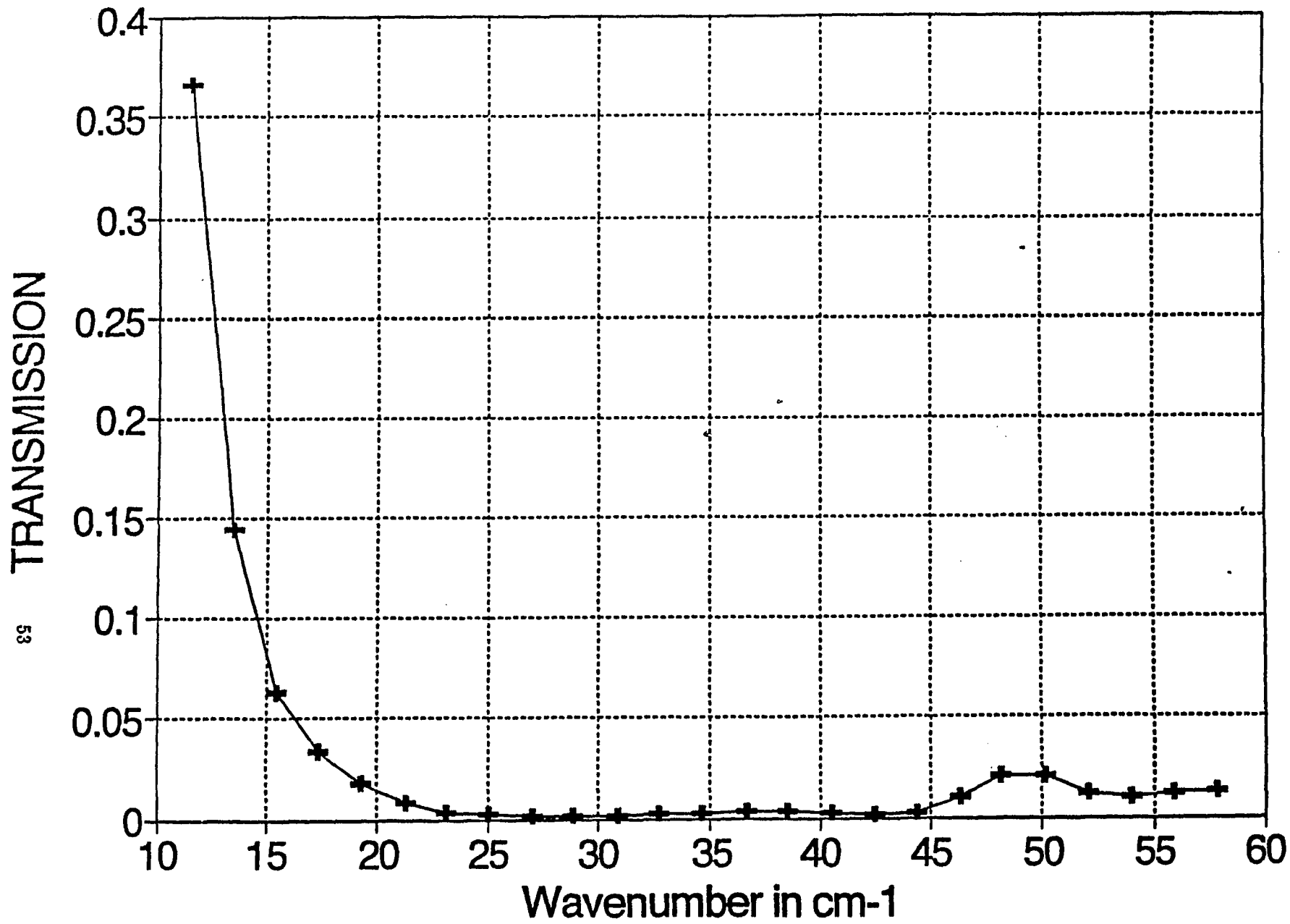


Fig. 4-9 THERMID Transmission Spectrum II

Wavenum	Transm.	Sample	Backgr.	Wavenum	Transm.	Sample	Backgr.
17.96875		0.000141	0.000221	11.5708	0.366077	37.79175	0.403259
17.1875		0.000202	0.000224	13.49927	0.143961	39.29688	1.066284
16.40625		0.000158	0.000142	15.42774	0.062855	34.51611	2.145081
15.625		0.000118	0.000271	17.3562	0.034057	27.73804	3.181519
14.84375		0.000214	0.000163	19.28467	0.017914	17.49658	3.815308
14.0625		0.000278	0.00025	21.21314	0.008042	7.761475	3.769989
13.28125		0.000254	0.000145	23.1416	0.003225	2.792725	3.382385
12.5		0.000173	0.000335	25.07007	0.001687	1.425537	3.300537
11.71875		0.000135	0.000426	26.99854	0.00093	0.916504	3.849365
10.9375		0.000217	0.000491	28.92701	0.000889	1.029541	4.525421
10.15625		0.000373	0.000509	30.85547	0.00126	1.530273	4.745453
9.375	0.432294	0.000332	0.000768	32.78394	0.001772	1.972656	4.349731
8.59375	0.440217	0.000404	0.000918	34.71241	0.002648	2.269287	3.347931
7.8125	0.32937	0.000291	0.000883	36.64087	0.003489	1.894531	2.121338
7.03125	0.500051	0.000568	0.001137	38.56934	0.003356	1.113281	1.295959
6.25	0.61566	0.000699	0.001136	40.49781	0.002437	0.623047	0.998657
5.46875	0.727988	0.000764	0.00105	42.42627	0.000904	0.216553	0.935791
4.6875	0.643032	0.0007	0.001088	44.35474	0.001933	0.437256	0.883667
3.90625	0.826738	0.001383	0.001673	46.28321	0.00986	1.820313	0.72113
3.125	0.607971	0.000517	0.000851	48.21168	0.020846	2.607666	0.488648
2.34375	0.870416	0.000575	0.000661	50.14014	0.020643	1.707275	0.323059
1.5625	1.326081	0.000514	0.000388	52.06861	0.011835	0.62207	0.205322
0.78125	1.511213	0.000391	0.000259	53.99708	0.01041	0.262695	0.098572
				55.92554	0.01184	0.164551	0.054291
				57.85401	0.013032	0.141113	0.042297

Table 4-1 Data of Fig.4-7 and Fig. 4-8

Table 4-2 Data of Fig. 4-9

## 4.5 Discussion

The study of molecular structures by spectrometry depends primarily on the existence of vibratory motions of atoms within the molecule. These motions depend on the nature and arrangement of the constituent atoms. Radiant energy, particularly infrared, falling upon matter is affected by the presence of such motions. A study of the behaviour of radiation falling upon matter is thus capable of giving indirect, but very valuable, information on molecular structure.

The far-infrared frequency range is the range extending from about  $300\text{ cm}^{-1}$  ( $33\ \mu$ ) out to the microwave region (millimetre and even centimetre waves). The principle energy levels involved in this range are of the order of a hundredth of an electron-volt, comparable to that of the thermal excitation of molecules at room temperature (  $0.03$  electron-volt). The results of the far infrared absorption experiments of the THERMID sample show that in the range of wave number  $1\text{ cm}^{-1}$  to  $25\text{ cm}^{-1}$ , the infrared absorption of the THERMID increases with the increasing of wave number and reaches the maximum at wave number  $25\text{ cm}^{-1}$ . In the range of wave number  $25\text{ cm}^{-1}$  to  $60\text{ cm}^{-1}$ , almost no transmission occurs. This means that some energy levels of THERMID molecules exist in this region. The energy levels of THERMID molecules that occur in this region owe their low frequency to several motions<sup>[19]</sup>: (1) The masses in movement are groups of atoms which move altogether with respect to the frame of the molecule; (2) The molecular chain has low frequency modes itself and one chain may move with respect to another; (3) Hydrogen bonds and Van der Waal forces produce weak bonds corresponding to motions of low frequencies; (4) Torsional vibrations of molecular groups and their tunneling may as well result in far infrared absorption.

Our far-infrared absorption measurements are not used to get the molecular structure of THERMID. The chemists of National Starch & Chemical Co. have already achieved this as shown in Fig. 2-13, and the absorption of greatest interest in polymer chemistry is associated with covalent bonds and occurs at frequencies in the middle infrared, from 4000 to 300  $\text{cm}^{-1}$ , corresponding to energy level differences of the order of 0.1 electron-volt. The results of our tests, however, will provide supplemental information for polymer chemists on the structure of THERMID and give us some bases of judgement for the potential future applications of THERMID in devices for the far-infrared region.

## Chapter 5 Summary

The progress of high performance electronic systems relies on the development of materials with improved properties. Acetylene-terminated polyimide oligomers, marked under the trade name THERMID, are receiving more and more attention from the microelectronics engineering because of their high thermal and chemical stability, low dielectric constants, excellent electrical insulation properties, and the simplicity of their processing. The study and evaluation of some of their electrical and optical properties in this thesis give more support to their application in the semiconductor industry, especially in the VLSI field.

In order to measure the very high bulk resistivity, surface resistivity, and breakdown voltage of THERMID EL-5010, a computer controlled test system, which includes an advanced Keithley 236 Source-Measure Unit and a special test fixture,

was designed and established. The sample preparation methods were carefully studied. We successfully measured the bulk resistivity, surface resistivity, and breakdown voltage of THERMID polyimide EL-5010 thin film dielectrics. The measurements were accomplished by actually fabricating microelectronic capacitor devices with the THERMID Film as the dielectric. The room temperature bulk resistivity of the THERMID EL-5010 films of 0.96  $\mu\text{m}$  to 2.56  $\mu\text{m}$  thicknesses was no less than  $1 \times 10^{16}$   $\Omega\text{-cm}$ . In the temperature range of 27°C to 160°C, the bulk resistivity was almost unchanged. When the temperature increased further, the bulk resistivity began to decrease and reached  $2 \times 10^{14}$   $\Omega\text{-cm}$  at 200°C. The room temperature breakdown voltage and the surface resistivity of the 1  $\mu\text{m}$  THERMID EL-5010 thin film were measured to be 350V and  $1 \times 10^{15}$   $\Omega/\square$  respectively.

The fixed charge concentration and mobile ion concentration in THERMID EL-5010 thin film were also obtained experimentally. These were accomplished using the technique of high frequency capacitance-voltage (C-V) measurements of metal-insulator-semiconductor (MIS) structure where THERMID was used as insulator layer. To ensure that the experiments were successful, extra attention was paid to sample preparations. The results of these experiments showed that there were  $10^{11}$   $\text{cm}^{-2}$  negative fixed charges in the THERMID EL-5010 thin film. The positive mobile ion concentration in the THERMID EL-5010 thin film was measured to be  $1.12 \times 10^{11}$   $\text{cm}^{-2}$ .

Far infrared absorption properties of THERMID polyimide EL-5010 over the wave number range of 1 - 60  $\text{cm}^{-1}$  were also studied in this thesis. In order to experimentally measure the far infrared absorption properties of THERMID EL-5010, a Fourier transform spectrometer, which includes a 250 watt mercury lamp, a

lamellar grating, and a dip-stick He-cooled detector, was set up. A special Fourier transformation program which adopts the Cooley - Turkey algorithm was used to untangle the "mixed" spectral elements produced by the lamellar grating spectrometer. The far infrared transmission properties of THERMID EL-5010 obtained by the lamellar grating spectrometer were over the wave number range of 1 - 10  $\text{cm}^{-1}$ . The transmission properties over the wave number range of 10 - 60  $\text{cm}^{-1}$  were obtained at Brookhaven National Laboratory where the synchrotron far infrared light source, a Nicolet Michelson scanning spectrometer, and a pumped He-cooled detector with  $10^{-14}$  NEP were used. The data obtained from the two systems matched very well and had a smooth transfer. These transmission spectra showed that in the wave number range of 1 - 25  $\text{cm}^{-1}$ , the infrared absorption of the THERMID EL-5010 increased with the increasing of wave number and reached the maximum at wave number 25 $\text{cm}^{-1}$ . In the wave number range of 25 - 60 $\text{cm}^{-1}$ , almost no transmission occurred.

Mechanisms responsible for resistivity, voltage breakdown, negative fixed charges, and far infrared absorption properties of THERMID polyimide are also suggested. Due to the limited experimental data at this time, these discussions are only preliminary.

For future work, the measurement and evaluation of the interface trap concentration at the THERMID polyimide-silicon interface, using the technique of pseudostatic state C-V characteristic measurement, should be done. A lamellar grating spectrometer installed in a vacuum chamber should be established. In this

way, the error caused by the water vapor absorption during the far infrared experiment can be eliminated. Finally, in order to get a better understanding of the mechanisms responsible for the electrical and optical properties of THERMID, more feedback between the measurement results and the fabrication of the THERMID polyimide are necessary.

## Reference

- [1] C.A.Harper and W.W.Staley, *Modern Electronic Packaging*, Sept.1989, p.58
- [2] R.R.Tummala and E.J.Rymazewski Ed., *Microelectronics Packaging Handbook*, New York, Van Nostrand Renhold, 1989, pp.38, 507
- [3] (A) Reche,J.J.H., *Circuits Manufacturing*, June 1989, pp.46-51  
(B) Licari,J.J., *Electronic Packaging and Production*, Sep.1989, pp.58-64
- [4] Tessier,T.G., Adema,G.M., and Turlik,T., "Polymeric Dielectric Options for Thin Film Packaging Applications", *ECC Proceedings*, May 1989, pp.127-134
- [5] (A) K.P.Shambrook and P.A.Trask, "High-Density Multichip Interconnect (HDMI)", *ECC Proceedings*, May 1989, pp.656-662  
(B) A.M.Wilson, "Polyimides Insulators for Multilevel Interconnections",*Thin Solid Films*, 83,1989, pp.145-163
- [6] Robert D.Rossi, "High Density Interconnect Packaging of Integrated Circuits Using A Polyimide Dielectric Interlayer", *Hybrid Circuit Technology*, Sep.1989, pp.35-39
- [7] *THERMID EL-5000 Series Polyimides*, National Starch & Chemical Co., P.O.Box 6500, Bridgewater, NJ 08807
- [8] W.Kern, *Semiconductor International*, August 1987, p.81
- [9] *Keithley 236 Source Measure Unit Applications Manual*, Keithley Instruments, Inc. Cleveland, Ohio, 1984, pp.2-8

- [10] A.R.Blythe, *Electrical Properties of Polymers*, Cambridge University Press, Cambridge,1980, p.90
- [11] R.W.Dyson, "Polymer Structures and General Properties", *Specialty Polymers*, Edited by R.W.Dyson, Chapman and Hall, New York, 1987, p.18
- [12] F.W.Billmeyer, *Textbook of Polymer Science*, QD381 .B52, 1984, p.347
- [13] N.A.Adrova etc., *Polyimides Progress in Material Science Series Vol. VI* TP1180 .P66, 1970, p.613
- [14] Michael Shur, *Physics of Semiconductor Devices*, Prentice-Hall Inc. A Division of Simon & Schuster, Englewood Cliffs, NJ.07632, 1990, pp.344-350
- [15] MM The Micromanipulator Co.,Inc. "Capacitance Analysis Programs", *C-V Operator Manual*, June 1988, p8.4
- [16] Guwei Len, *Si- SiO<sub>2</sub> Interface Physics*, Defence Industry Publication of P.R.China, 1984
- [17] K.D.Moller, *Optics*, University Science Books, Mill Valley, CA. 1988, pp331-339
- [18] R.Bell, *Introductory Fourier Transform Spectroscopy*, Academic Press, 1972, pp237-250
- [19] R.G.Zoeller, N.G.Ugras and K.D.Moller, "Fourier Transform Spectrometer for the 1 to 10 mm Region", *Int.J. of Infrared and Millimeter Waves*, Vol.9,1988, pp45-49

## Appendix

### Appendix A : Program for THERMID Resistivity Measurement

```
10 DECLARE SUB PLOTTER 'ref. to BASIC sub "plotter"
20 DECLARE SUB SCREENMODE ' "screenmode" and "graphxy"
30 DECLARE SUB GRAPHXY
40 OPEN "\DEV\IEEEOUT" FOR OUTPUT AS #1 ' open IEEE-48 output path
50 OPEN "\DEV\IEEEIN" FOR INPUT AS #2 ' open IEEE-48 input path
60 IOCTL #1, "BREAK" ' reset interface
70 PRINT #1, "RESET" ' warm start interface
80 PRINT #1, "CLEAR" ' send device clear
90 PRINT #1, "REMOTE 16" ' put 236 in remote
100 CLS
110 OPTION BASE 1
120 DIM RX(901), RY(901), RT(901), V(50), I(50), R(50), P(50)
130 INPUT "DATE: MONTH/DAY/YEAR"; DDAT$
150 PRINT "FILM DIA.=?(CM),FILM THICK=?(CM),TEMP.=?(K)"
160 INPUT D, L, T
170 PRINT #1, "OUTPUT 16;FO,1X" ' source V, measure I, sweep mode
180 PRINT #1, "OUTPUT 16;O0T1,0,0,0X" ' local sense, trigger on GET
190 PRINT #1, "OUTPUT 16;L1E-3,0X" ' 1MA compliance, AUTO range
200 PRINT #1, "OUTPUT 16;G5,2,1X" ' source, measure, no prefix,sweep data
210 PRINT #1, "OUTPUT 16;S2P5M2,X" ' 60Hz ac, 5-dig. reso., filler=32,
220 PRINT #1, "OUTPUT 16;B0,0,0X" ' program 0 bias value
230 PRINT #1, "OUTPUT 16;Z0X" ' disable suppression
240 PRINT #1, "OUTPUT 16;Q0,0,0,30000,10X" ' create ov level sweep(discharge sample)
250 INPUT "STA.VOLT=?(V),END VOLT=?(V),STEP=?"; M,N,S
270 FOR V = M TO N STEP S ' append a series of fixed level sweep
280 PRINT #1, "OUTPUT 16;Q6,?; V; ",0,30000,10X" ' these point used as delay(5 min.)
290 PRINT #1, "OUTPUT 16;Q6,?; V; ",0,100,10X" ' these points used as data(10 points)
300 NEXT V
310 PRINT "CLOSE LID, PRESS ANY KEY TO BEGIN."
```

```

320 DO WHILE INKEY$ = " ": LOOP
330 PRINT #1, "UOUTPUT 16;RINIX"           ' Arm sweep, turn on 236 output
340 PRINT #1, "TRIGGER 16"               ' trigger sweep
350 PRINT #1, "STATUS"                   ' get bus status
360 INPUT #2, ST$                         ' input status string
370 IF MID$(ST$, 11, 2) = "SO" THEN GOTO 350 ' wait for SRQ
380 PRINT #1, "SPOLL 16"                  ' serial poll 236 to clear SRQ
390 INPUT #2, SB
400 PRINT #1, "OUTPUT 16;NOX"             ' turn off 236 output
410 X1 = (N - M) / S + 1
420 X = 10 + 20 * X1                       ' total number of meas. point
430 FOR I = 1 TO X
440 PRINT #1, "ENTER 16"                  ' address 236 to talk
450 INPUT #2, RX(I), RY(I)                ' input current and voltage readings
460 NEXT I
470 CLOSE 1: CLOSE 2
480 IO = 0#                                ' find current at 0V
490 FOR I = 1 TO 10
500 IO = RY(I) + IO
510 NEXT I
520 IO = IO/10                             ' "zero point" compensation
530 FOR I = 11 TO X
540 RY(I) = RY(I) - IO
550 NEXT I
560 RT(1) = 0
570 FOR I = 2 TO X
580 RT(I) = (I-1) * 100 * 160             ' delay coef.(=160) for data acqui.
590 NEXT I
600 PRINT TAB(4); "VOLT(V)"; TAB(20); "CUR.(A)"; TAB(40);
610 PRINT "R(OM)"; TAB(60); "p(OM-CM)"
620 X$ = STRING$(20, 61)
630 LPRINT TAB(10); X$; "DATA OF THERMID DC MEAS."; X$
640 LPRINT: LPRINT
650 LPRINT TAB(10); "DATE:"; TAB(31); DDAT$

```

```

660 LPRINT TAB(10); "FILM THICK: "; TAB(30); L; "(CM)"
670 LPRINT TAB(10); "DIAM. OF MEAS. : "; TAB(30); D; "(CM)"
680 LPRINT TAB(10); "TEMP. UNDER TEST: "; TAB(30); T; "(K)"
690 LPRINT: LPRINT
700 LPRINT TAB(4); "VOLT(V)"; TAB(20); "CUR.(A)"; TAB(40);
710 LPRINT "RESIST.(OM)"; TAB(60); "RESISTIVITY(OM-CM)"
720 X$ = STRING$(80, 45)
730 LPRINT X$
740 FOR J = 1 TO X1 ' current points used to plot V-I curve
750 I(J) = 0
760 FOR K = 1 TO 10 ' these points used for delay
770 A = 20 * J + K
780 I(J) = I(J) + RY(A)
790 NEXT K
800 I(J) = I(J)/10
810 NEXT J
820 SUMp = 0#
830 FOR K = 1 TO X1 ' voltage points used to plot V-I curve
840 V(K) = M + (K - 1) * S
850 R(K) = V(K)/I(K)
860 p(K) = R(K) * 3.14159 * ((D/2)^2)/L ' resistivity of each points
870 PRINT TAB(4); V(K); TAB(20); I(K); TAB(40); R(K);
880 PRINT TAB(60); p(K)
890 LPRINT TAB(4); V(K); TAB(20); I(K); TAB(40); R(K);
900 LPRINT TAB(60); p(K)
910 SUMp = SUMp + p(K) ' find average resistivity of THERMID
920 NEXT K
930 AVEp = SUMp/X1
940 PRINT:PRINT "RESISTIVITY = " AVEp
950 X$ = STRING$(80,45)
960 LPRINT X$: LPRINT: LPRINT
970 X$ = STRING$(3, 42)
980 LPRINT TAB(7); X$; TAB(11);
990 LPRINT "BULK RESISTIVITY OF THERMID: "; TAB(42);

```

```

1000 LPRINT AVEp; "OM-CM"; TAB(65); X$
1010 PRINT "PRESS KEY TO DISPLAY HRAPH"
1020 DO WHILE INKEY$ = " ": LOOP
1030 TITLE$ = "THERMID DC MEAS. V-I CURVE"
1040 CALL SCREENMODE (16)
1050 SCREEN
1060 N% = X1
1070 CALL PLOTTER (1)
1080 CALL GRAPHXY(SEG V(1), SEG I(1), N%, 1, "VOLT.(V)", 1, "I(A)", TITLE$, 1, 1, 2)
                                     ' display V-I curve on screen
1090 PRINT "DO YOU WANT TO PLOT V-I CURVE?(Y/N)"
1100 INPUT A$
1110 IF MID$(A$, 1, 1) = "Y" THEN GOTO 1120 ELSE
      IF MID$(A$, 1, 1) = "N" THEN GOTO 1140 ELSE
      GOTO 1100
1120 CALL PLOTTER(2, 1, 0)
1130 CALL GRAPHXY(SEG V(1), SEG I(1), N%, 1, "VOLT.(V)", 1, "I(A)", TITLE$, 1, 1, 2)
                                     ' plot V-I curve
1140 CLS: TITLE$ = "THERMID DC MEAS. T-V CURVE"
1150 M% = X
1160 CALL PLOTTER(1)
1170 CALL GRAPHXY(SEG RT(1), SEG RX(1), M%, 1, "T(MSEG)", 1, "VOLT.(V)", TITLE$, 1, 0, 2)
1180 PRINT "DO YOU WANT TO PLOT T-V CURVE?(Y/N)"
1190 INPUT B$
1200 IF MID$(B$, 1, 1) = "Y" THEN GOTO 1210 ELSE
      IF MID$(B$, 1, 1) = "N" THEN GOTO 1230 ELSE
      GOTO 1190
1210 CALL PLOTTER(2, 1, 0)
1220 CALL GRAPHXY(SEG RT(1), SEG RX(1), M%, 1, "T(MSEG)", 1, "VOLT(V)", TITLE$, 1, 0, 2)
1230 CLS: TITLE$ = "THERMID DC MEAS. T-I CURVE"
1240 CALL PLOTTER(1)
1250 CALL GRAPHXY(SEG RT(1), SEG RY(1), M%, 1, "T(MSEC)", 1, "I(A)", TITLE$, 1, 0, 2)
1260 PRINT "DO YOU WANT TO PLOT T-I CURVE?(Y/N)"
1270 INPUT C$

```

```
1280 IF MID$(C$, 1, 1) = "Y" THEN GOTO 1290 ELSE
      IF MID$(C$, 1, 1) = "N" THEN GOTO 1310 ELSE
      GOTO 1270
1290 CALL PLOTTER(2, 1, 0)
1300 CALL GRAPHXY(SEG RT(1), SEG RY(1), M%, 1, "T(MSEG)", 1, "I(A)", TITLE$, 1, 0, 2)
1310 END
```

## Appedix B: Program for THERMID Far-Infrared Absorption Properties Measurement

```
10 DECLARE SUB PLOTTER 'reference to BASIC sub: "PLOTTER",
20 DECLARE SUB SCREENMODE ' "SCREENMODE", "GRAPHXY"
30 DECLARE SUB GRAPHXY
40 CLEAR , . 1024
50 DIM X(300), Y(300),
60 CLS
70 SCREEN 2
80 PRINT " ACQUIRE NEW SPECTRUM (1) OR PLOT OLD (2) ?"
90 INPUT CHOICE
100 IF CHOICE = 1 THEN GOTO 130 'obtain new interferogram
110 IF CHOICE = 2 THEN GOTO 4000 , plot old interferogram
120 GOTO 80
130 INPUT "FILE NAME FOR DATA"; F$
140 IF F$ = " " THEN PRINT "YOU MUST ENTER A FILENAME": GOTO 130
150 IF INSTR(1, F$, ".") = 0 THEN F$ = F$ + ".PRN"
160 INPUT "HOW MANY POINTS ?"; S% ' sample points of test
170 IF S% <= 0 THEN PRINT "AT LEAST ONE SAMPLE ": GOTO 160
180 INPUT " HOW LONG TO WAIT BETWEEN SAMPLE"; D%waiting time between two samples
190 IF D% <= 0 THEN PRINT " MUST BE > 0": GOTO 180
200 OPEN "COM1: 1200, N, 7, 1, CS, DS, RS" FOR RANDOM AS #1
210 PRINT #1, "S9" ' set string length: 9 records per string
220 X(0) = 0 ' to WHITE BOX
230 FOR SMPLCNT = 1 TO S%
231 X(SMPLCNT) = X(SMPLCNT - 1) + D%
232 NEXT SMPLCNT
233 FOR SMPLCNT = 1 TO S%
240 GOSUB 1000 ' sample subroutine
241 CALL SCREENMODE(16) ' display interogram curve during test
242 SCREEN 1
243 TITLE$ = " INTERFEROGRAM CURVE"
244 CALL PLOTTER(1)
```

```

250 CALL GRAPHXY(SEG X(1), SEG Y(1), S%, 1, "OPT. PATH DIFF", 1, "RELATIVE INTENSITY",
      TITLES$, 1, 0, 2)
260 NEXT SMPLCNT
270 CLOSE 1: OPEN F$ FOR OUTPUT AS #1           ' store test data in file named as F$
280 FOR SMPLCNT = 1 TO S%
290 PRINT #1, SMPLCNT, Y(SMPLCNT), 0
300 NEXT SMPLCNT
310 CLOSE #1
320 BEEP: BEEP:
330 GOTO 5000
1000 PRINT #1, "OXXX0"                         ' instruction: "turn off" step motor
1010 TD% = 1: GOSUB 3000                        ' delay 1 second
1020 PRINT #1, "OXXX1"                         ' instruction: "turn on" step motor
1030 TD% = D%                                  ' waiting D seconds
1040 GOSUB 3000
1050 PRINT #1, "C": PRINT #1, "E"             ' start A/D conversion and
1060 WHILE LOC(1) <> 9                          ' stop conversion at end of record
1070 WEND                                       ' obtain one sample point data
1080 D$ = INPUT$(LOC(1), 1)
1090 Y(SMPLCNT) = VAL(D$)
1100 RETURN
3000 FOR TDC = 1 TO D%                          ' "DELAY" subroutine
3010 FOR TDC1 = 1 TO 5000: NEXT TDC1
3020 NEXT TDC
3030 RETURN
4000 INPUT "FILE NAME TO BE PLOTTED"; F2$     ' input old interferogram named as F2$
4010 OPEN F2$ FOR INPUT AS #1
4020 J = 0
4030 WHILE (NOT (EOF(1)))
4040 J = J + 1
4050 INPUT #1, X(J), Y(J), JUNK2
4060 WEND
4070 CALL SCREENMODE(16)                       ' display the old interferogram curve
4080 SCREEN 1

```

```

4090 TITLE$ = "THE INTERFEROGRAM CURVE"
4095 S1% = J
4100 CALL PLOTTER(1)
4110 CALL GRAPHXY(SEG X(1), SEG Y(1), S1%, 1, "RELATIVE OPT. PATH DIFF", 1,
    "RELATIVE INTENSITY", TITLE$, 1, 0, 2)
4120 INPUT "DO YOU WANT TO PLOT THE GRAPH?(Y/N)"; A$
4130 IF MID$(A$, 1, 1) = "Y" THEN GOTO 4200 ELSE
    IF MID$(A$, 1, 1) = "N" THEN GOTO 320 ELSE GOTO 4120
4200 CALL PLOTTER(2, 1, 0) ' plot the old interferogram curve
4210 CALL GRAPHXY(SEG X(1), SEG Y(1), S1%, 1, "RELATIVE OPT. PATH DIFF.", 1,
    "RELATIVE INTENSITY", TITLE$, 1, 0, 2)
4220 GOTO 320
5000 INPUT "NOW, DO YOU WANT FFT/IFT? (Y/N)"; A$ ' perform Fourier transform using
5010 IF MID$(A$, 1, 1) = "Y" THEN GOTO 5020 ELSE ' Cooley-Turkey algorithm
    IF MID$(A$, 1, 1) = "N" THEN GOTO 6210 ELSE GOTO 5000
5020 CLS
5030 INPUT "DATE"; DA$
5040 INPUT "HR"; HR$
5050 INPUT "FWD-OR-INV?(F/I)"; AN$
5060 IF AN$ = "F" THEN D=0 ELSE
    IF AN$ = "I" THEN D=1 ELSE GOTO 5050
5080 INPUT "M=? (HERE 2^M=1/2 SAMPLE NUMBER)"; M
5090 N = 2^M
5100 PRINT "N="; N
5110 DIM X(2*N + 20, 2), C(2*N + 30), CC(2*N + 30), B(2*N + 30), A(N + 20)
5160 IF D=0 THEN PRINT "INPUT TIME DOMAIN DATA"
5170 IF D=1 THEN PRINT "INPUT FREQ. DOMAIN DATA"
5180 INPUT " ENTER [*.PRN]"; F$ ' input interferogram data that needed
5190 OPEN F$ FOR INPUT AS #1 ' to be transformed
5210 FOR G=1 TO N+14 STEP 1
5220 INPUT #1, JUNK, C(G), A
5230 NEXT G
5240 FOR G=1 TO N+14 ' 5240-5530: Cooley-Turkey Algorithm
5250 Z=C(1)+C(2)+C(3)+C(4)+C(5)+(6)+C(7)+C(8)+C(9)+C(10)

```

```

5260 U=C(N+5)+C(N+6)+C(N+7)+C(N+8)+C(N+9)+C(N+10)+C(N+11)+C(N+12)+C(N+13)+C(N+14)
5270 ZZ=(Z-U)/(10*(N+14-10))
5280 CC(G)=C(G) + ZZ*G
5290 NEXT G
5300 MAX=0: MAXIND=0
5320 FOR I=1 TO N+14
5330 IF CC(I) > MAX THEN MAX=CC(I): MAXIND=I
5340 NEXT I
5350 PRINT CC(MAXIND)
5360 LET P= MAXIND: PRINT P
5370 FOR G=1 TO N
5380 LET B(G)=CC(P-(N/2)+G)
5390 NEXT G
5400 FOR G=1 TO N
5410 LET V=(B(1)+B(2)+B(3)+B(4)+B(5)+B(6))/6
5420 LET W=(B(N)+B(N-1)+B(N-2)+B(N-3)+B(N-4)+B(N-5)+B(N-6))/6
5430 H=(V+W)/2
5440 A(G)=B(G)-H
5450 NEXT G
5460 FOR G=1 TO N/2
5470 X(G,0)=A((N/2)+G)
5471 X(G,1)=0
5480 NEXT G
5481 FOR G=1 TO 5
5483 NEXT G
5490 FOR G=(N/2)+1 TO N
5500 X(G,0)=A(G-(N/2))
5510 X(G,1)=0
5520 NEXT G
5521 FOR G=N-5 TO N
5523 NEXT G
5530 CLOSE 1: OPEN "O", #2, "FTIN5.PRN"
5540 FOR G=1 TO N
5550 PRINT #2, ; G; " "; X(G,0); " ": X(G,1)

```

*'data before fourier transform*

```

5560 NEXT G
5570 GOSUB 6230
5580 PRINT "/////////"
5590 IF D=0 THEN PRINT "NOW IN FREQ. DOMAIN"
5600 DIM XX(2*N+20,2)
5605 INPUT "ENTER OUTPUT [* .PRN]"; G$
5610 PRINT "XFRMD DATA IS:"
5620 PRINT "POINT      REAL      IMAG"
5630 PRINT
5650 PRINT
5680 PRINT
5700 CLOSE 2 : OPEN G$ FOR OUTPUT AS #3
5710 DIM R(N), RR(N)
5730 FOR I=1 TO N/2
5740 XX(I,0)=X(N/2 + I,0)
5750 XX(I,1)=X(N/2 + I,1)
5760 R(I)=(XX(I,0))^2+(XX(I,1))^2
5770 RR(I)=SQR(R(I))
5780 PRINT #3, ; I; " "; XX(I,0); " "; XX(I,1); " "; RR(I)
5790 NEXT I
5800 FOR I=(N/2) + 1 TO N
5810 XX(I,0) = X(I-(N/2),0)
5820 XX(I,1)=X(I-(N/2),1)
5830 R(I)=(XX(I,0))^2+(XX(I,1))^2
5840 RR(I)=SQR(R(I))
5850 PRINT #3, ; I; " "; XX(I,0); " "; XX(I,1); " "; RR(I)
5860 NEXT I
5870 MAX=0
5880 MAXIND=0
5890 FOR J=1 TO N/2
5900 IF RR(J)>MAX THEN MAX=RR(J): MAXIND=J
5910 NEXT J
5920 PRINT RR(MAXIND)
5930 DEFINT K

```

*'go for Fourier Transform*

*'non normalized spectrum data:*

*'I--rela. wave num.; RR(I)-- rela.intensity*

```

5940 DIM K(N)
5950 FOR I=1 TO (N/2)
5960 K(I)=(65*RR(I)/(RR(MAXIND)))
5970 DEFINT K
5980 NEXT I
5990 INPUT "INPUT HIGHEST WAVE NUMBER"; H
6010 FOR I =1 TO (N/2)
6020 F=I*H/(N/2)
6030 PRINT
6050 FOR Z=0 TO 70
6060 IF Z<>0 THEN GOTO 6120
6070 PRINT (H-F);
6100 IF K(I)>0 THEN GOTO 6150
6110 GOTO 6180
6120 IF Z=K(I) THEN GOTO 6160
6130 PRINT " ";
6150 NEXT Z
6160 PRINT I;"*";
6180 NEXT I
6190 PRINT
6200 PRINT "====="
6210 PRINT "      -DONE-"
6220 END
6230 REM*****
6240 REM FFT/IFT SUBROUTINE
6250 REM*****
6260 N=2*M
6280 N2=N/2
6290 N1=N-1
6300 J=1
6310 FOR I=1 TO N1
6320 IF I>=J THEN GOTO 6390
6330 T1=X(J,0)
6340 T2=X(J,1)

```

*'normalized intensity*

*'5990-6160:calculate wave number &*

*' display normalized spectrum:*

*, " Wave num. - Relative Intensity"*

*'do bit shuffle*

```

6350 X(J,0)=X(I,0)
6360 X(J,1)=X(I,1)
6370 X(I,0)=T1
6380 X(I,1)=T2
6390 K=N2
6400 IF K>=J THEN 6440
6410 J=J-K
6420 K=K/2
6430 GOTO 6400
6440 J=J+K
6450 NEXT I
6470 S1=-1
6480 IF D=0 THEN 6500
6490 S1=1
6500 P1=3.1415926535898#
6510 FOR L=1 TO M
6520 L1=2*L
6530 L2=L1/2
6550 U2=0
6560 W1=COS(P1/L2)
6570 W2=S1*SIN(P1/L2)
6580 FOR J=1 TO L2
6590 FOR I=J TO N STEP L1
6600 I1=I+L2
6620 V1=(X(I1,0)*U1-X(I1,1)*U2)
6630 V2=(X(I1,1)*U1+X(I1,0)*U2)
6640 X(I1,0)=X(I,0)-V1
6650 X(I1,1)=X(I,1)-V2
6660 X(I,0)=X(I,0)+V1
6670 X(I,1)=X(I,1)+V2
6680 NEXT I
6700 U3=U1
6710 U4=U2
6720 U1=(U3+W1-U4+W2)

```

*'end of shuffle*

*' do Butterfly*

*' do Twidl factor*

```
6730 U2=(U4+W1+U3+W2)
6740 NEXT J
6750 NEXT L
6760 IF D=1 THEN 6810
6770 FOR I=1 TO N
6780 X(I,0)=X(I,0)/N
6790 X(I,1)=X(I,1)/N
6800 NEXT I
6810 RETURN
```